AD_____

Award Number: W81XWH-10-1-0031

TITLE: Early Detection of Breast Cancer Using Posttranslationally Modified Biomarkers

PRINCIPAL INVESTIGATOR: Hongjun Jin

CONTRACTING ORGANIZATION: Battelle Memorial Institute
Richland, WA 99354

REPORT DATE: September 2013

TYPE OF REPORT: Annual Summary

PREPARED FOR: U.S. Army Medical Research and Materiel Command
Fort Detrick, Maryland 21702-5012

REPORT DOCUMENTATION PAGE

Form Approved
OMB No. 0704-0188

1. REPORT DATE *(DD-MM-YYYY)*	2. REPORT TYPE	3. DATES COVERED *(From - To)*
September 2013	Annual Summary	1 March 2012 - 30 August 2013

4. TITLE AND SUBTITLE
Early Detection of Breast Cancer Using Posttranslationally Modified Biomarkers

5a. CONTRACT NUMBER

5b. GRANT NUMBER
W81XWH-10-1-0031

5c. PROGRAM ELEMENT NUMBER

6. AUTHOR(S)
HONGJUN JIN

E-Mail: hongjunj@mir.wustl.edu

5d. PROJECT NUMBER

5e. TASK NUMBER

5f. WORK UNIT NUMBER

7. PERFORMING ORGANIZATION NAME(S) AND ADDRESS(ES)
Battelle Memorial Institute
Richland, WA 99354

8. PERFORMING ORGANIZATION REPORT NUMBER

9. SPONSORING / MONITORING AGENCY NAME(S) AND ADDRESS(ES)
U.S. Army Medical Research and Materiel Command
Fort Detrick, Maryland 21702-5012

10. SPONSOR/MONITOR'S ACRONYM(S)

11. SPONSOR/MONITOR'S REPORT NUMBER(S)

12. DISTRIBUTION / AVAILABILITY STATEMENT
Approved for Public Release; Distribution Unlimited

13. SUPPLEMENTARY NOTES

14. ABSTRACT

In this project, we focus on oxidation and glycosylation PTMs on proteins known to be secreted by the breast as candidate biomarkers for the early detection of breast cancer. ELISA microarray technology has employed to evaluate assays that have potential be used as breast cancer biomarkers. During the third year of this project we have continued the validation for our PTM-ELISA microarray. And we validated the chosen PTM antibody for pre-clinical or translational molecular imaging studies. The microPET imaging suggested that those PTM antibodies have high specific accumulation for breast cancer in tumor xenograft mice. Overall, our data suggest that the PTM ELISA microarray platform is a promising tool for discovery and evaluation of biomarkers that have potential for the early detection of breast cancer.

15. SUBJECT TERMS
ELISA, microarray, Post-translationally modifications(PTMs)

16. SECURITY CLASSIFICATION OF:			17. LIMITATION OF ABSTRACT	18. NUMBER OF PAGES	19a. NAME OF RESPONSIBLE PERSON
a. REPORT	b. ABSTRACT	c. THIS PAGE			USAMRMC
U	U	U	UU	50	19b. TELEPHONE NUMBER *(include area code)*

Table of Contents

Introduction

Early breast cancer detection is to find cancers before they start to cause symptoms. Mammography is the current standard test for breast cancer screening although many false positive results have been reported (*1*, *2*). Magnetic resonance imaging (MRI) is also recommended along with mammograms for some women at high risk for breast cancer. Ultrasound and other tests may also be helpful for some women. Current screening methods, including clinical breast examination and conventional mammography, have high rates of false-positive and false negative results (*3-6*). Positron Emission Tomography (PET**)** is a newly developed imaging tool for early detection of cancers including the breast cancer. PET is a great non-invasive imaging method that measure the biochemical functional cellular biomarkers in living subjects. PET can detect breast cancer before it can be seen with mammograms and may be as good as or better than breast MRI. In this postdoctoral fellowship investigation we screened several post-translational protein modifications (PTMs) that are potentially characteristic of early breast cancer using ELISA microarray. And in the last year of the continuation studies, we validated one of these selected antibodies for PET imaging studies on tumor xenograft mouse.

Body

Oxidative PTMs Oxidative stress is transiently increased in breast cancer development and progression (*7-9*). Studies on human breast cancer have suggested that this increase in oxidative stress is greatest in the early stages of the disease (*8, 9*). This stress would be expected to

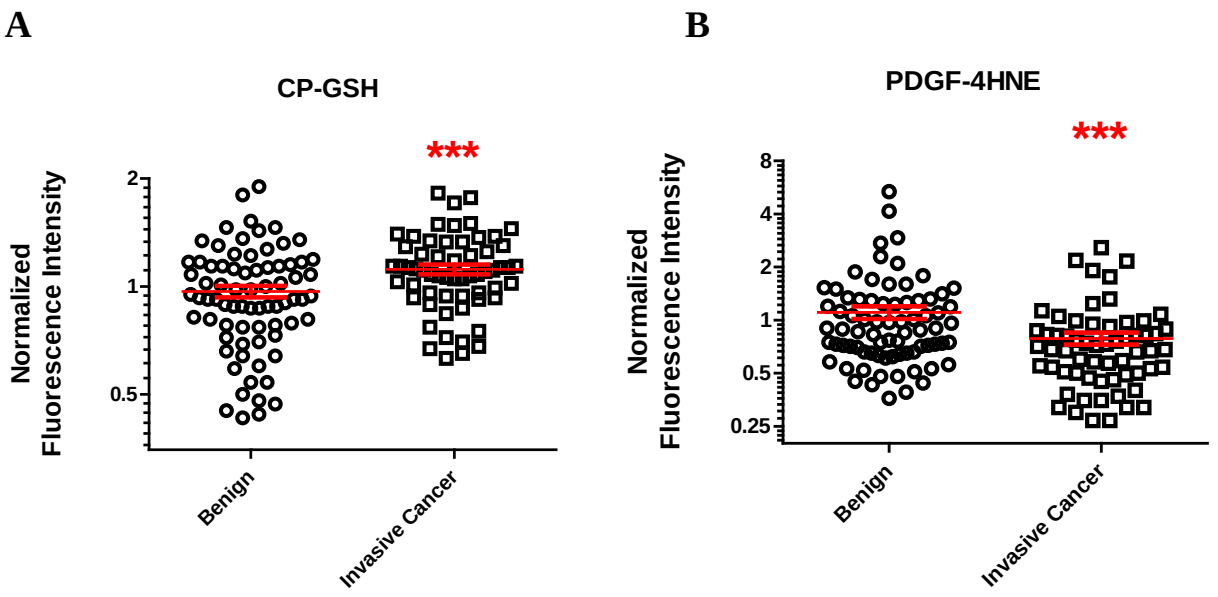

Figure 1. Representative graphs of normalized fluorescence data for oxidative modifications in individual proteins found in plasma. Each data point represents the average raw fluorescence signal for triplicate analyses (one chip per analysis) of a single sample. The ANOVA model included a two-level study factor to account for intensity offsets between studies while the intensities were Box-Cox transformed in order to produce normally distributed residuals of the same scale between studies. **A** .CP-GSH, glutathionylated ceruloplasmin; **B**. PDGF-4HNE, 4-hydroxynonenal-adducted platelet-derived growth factor. Each data point shown here represents data derived from 12 analyses. The bar in the figure represent the mean and the standard errors. The star denote that the mean value from invasive cancer are significant different from the benign samples (P value was less than 0.05 by t-tests).

increase the oxidative modification of proteins that are secreted into the blood. In this study, we evaluate oxidative, post-translational protein modifications (PTMs) that are potentially characteristic of early breast cancer. Because we expect the modified proteins to be at low abundance, we use the sandwich enzyme-linked immunosorbent assays (ELISAs) because these assays have exceptional sensitivity and specificity. In the sandwich ELISA, one antibody is used to capture and concentrate the target protein and a second antibody selectively measures the oxidative modification.

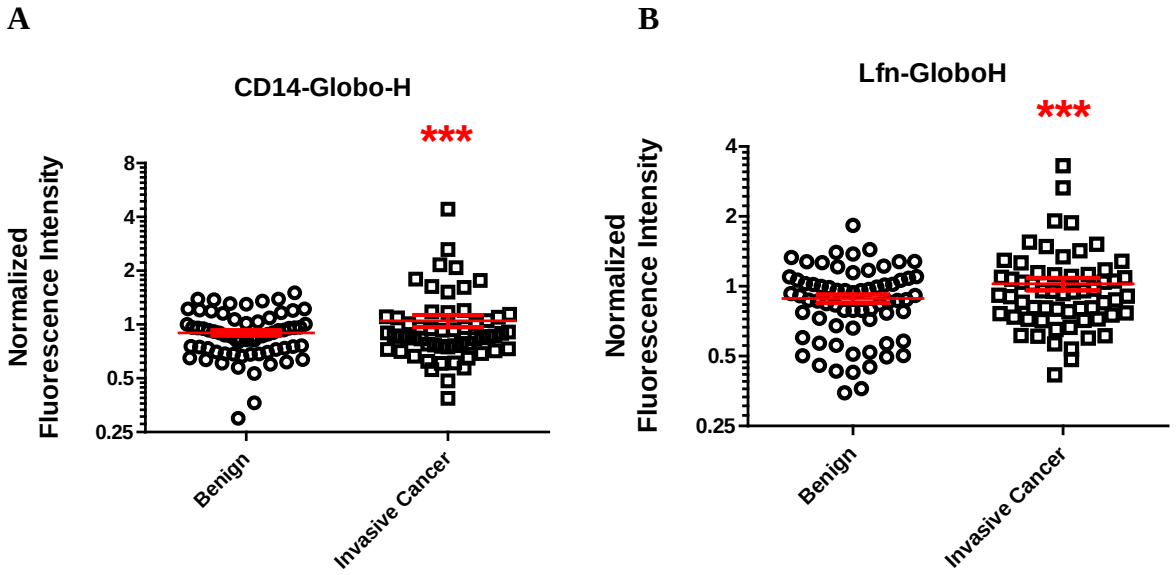

Figure 2. Representative graphs of normalized fluorescence data for Globo-H modifications in individual proteins found in plasma. A. CD14-Globo-H**:** Globo-H modified CD14; **B.** Lfn-Globo-H, Globo-H modified lactoferrin. The bar in the figure represent the mean and the standard errors. The star denote that the mean value from invasive cancer are significant different from the benign samples (P value was less than 0.05 by t-tests).

Develop and validate oxidative PTM-ELISA microarray We validated our PTM-ELISA microarry with two groups of human plasma samples collected from Duke University for a total of 160 subjects. As we stated in our proposal, we have evaluated oxidation modifications using the new PTM microarray chip. For oxidative modifications, 4-hydroxynonenal (4HNE), nitrotyrosine, and glutathione (GSH) adducts were tested with commercial available antibodies and antigens to select the best specificity and sensitivities. These modifications could be associated with oxidative stress for the immune response (*8*, *9*). When we established this PTM-ELISA microarray assay, and tested with breast cancer plasma samples, we found 4HNE protein modification is alerted early breast cancer with several circulating proteins (i.e. PDGF, HGF) (Figure 1). Glutathione (GSH) is protein adduct which is an indicative of intracellular oxidative stress, especially in the endoplasmic reticulum. Growing evidence suggested that GSH adducts is useful indictor of breast cancer (*10*-*12*). Our results suggest that oxidatively modified proteins are altered in plasma from breast cancer patients and that these proteins have potential to be used as biomarkers for this disease.

Glycosylation PTMs Cancer cells can express high levels of certain tumor-associated carbohydrate antigens (TACA). These structural changes can alter cellular function, including adhesive properties and potential to invade and metastasize. We developed Globo-H-ELISA microarray assays, and tested it with clinical breast cancer samples. We found several circulating proteins containing this modification are altered in invasive cancer (Figure 2). Based on the development of these methods, we published one method paper on Cancer Biomarker. (Appendix).

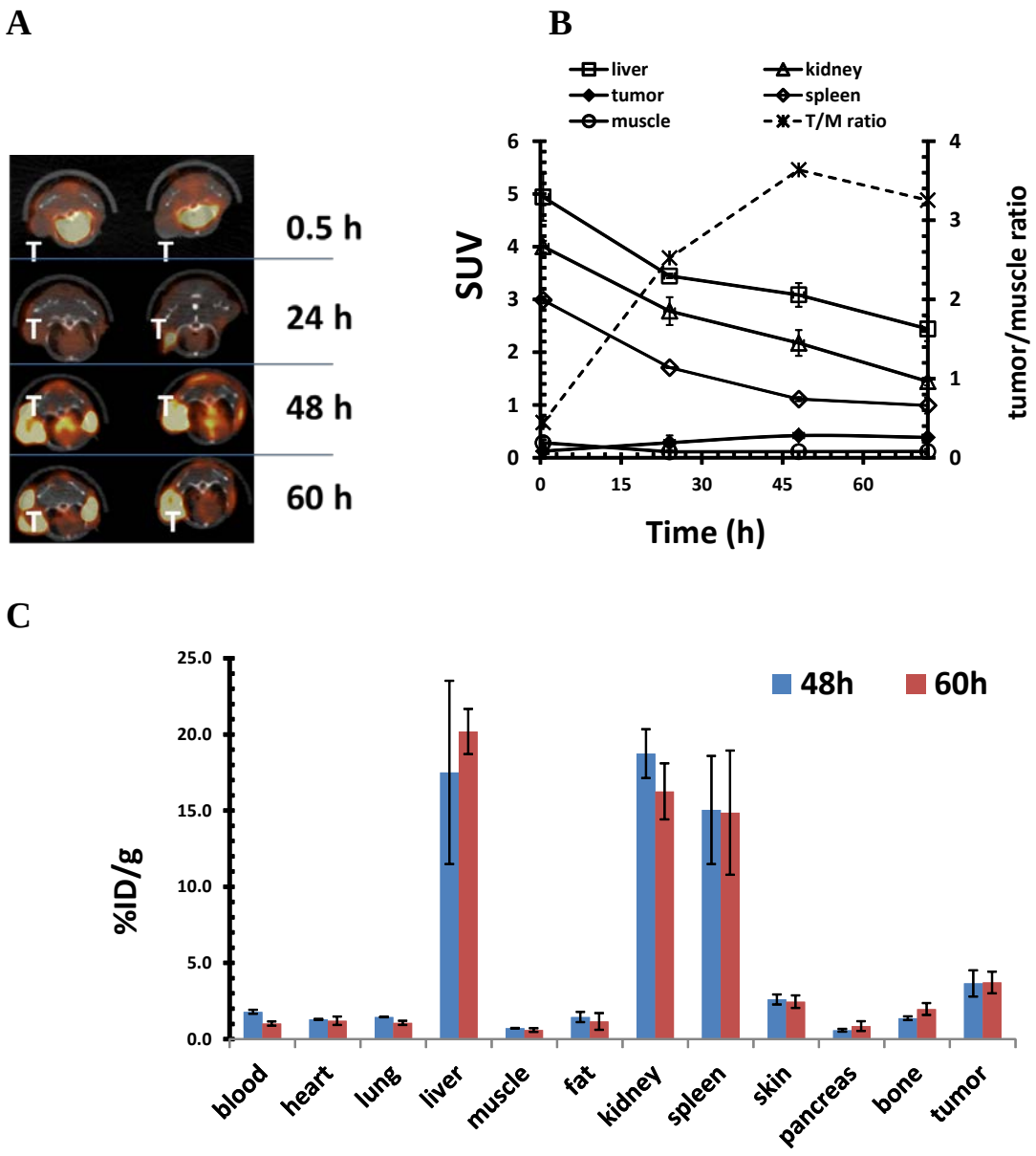

Figure 3 Molecular imaging studies for Globo-H antibody ^{89}Zr-labeled anti-Globo-H antibody was administrated (i.v.) to the MCF-7 tumor xenograft mouse. **A**). The transverse section of the microPET images from post injection of 0.5, 24, 48 and 60 h. B). Tissue activity curve was produced from post injection of statics microPET images from MCF-7 tumor xenograft mouse (n=2). C. Biodistribution of ^{89}Zr-anti-Globo-H in MCF-7 tumor xenograft mouse for post injection 48 h (n=4) and 60 h (n=4) .

GloboH antibody microPET imaging studies Because glycosylation of cancer-related biomarkers can be determined using specific antibody, we hypothesized that antibodies against specific glycosylation would be valuable in cancer detection *in vivo*. Encouraged by the PTM-ELISA screening result, we decided to explore the microPET imaging studies for the selected PTM antibodies. For establishing the methods, one novel glycosylation antibody, named Mab H6-11 was successfully conjugated with the chelator p-SCN-Bz-DFO and labeled with ^{89}Zr PET radioisotope with 97% radiochemical yield (Appendix). For Globo-H antibody microPET imaging studies, at different time points post injection of ^{89}Zr-p-SCN-Bz-DFO-anti-Globo-H, the microPET scans were performed on MCF-7 tumor xenograft mice. The microPET imaging

showed that the radioactivity uptake gradually increased in the tumor tissue and decrease in the liver at 48-60 h post injection (Figure 3A). The tumor imaging lasted at least 60 h post injection where the tumor to muscle ratio reached as high as 3.5 (Figure 3B). The biodistribution result also suggested that the radiolabeled antibody showed specific uptake (4 ID%/g) to the breast cancer tumor (Figure 3C). This result is very encouraging for further pre-clinical or translational investigation. Our study suggested that PTM-ELISA screened antibodies can be applied directly for the non-invasive PET imaging for breast cancer early detection.

Progress according to our Specific Aims and Statement of Work

Specific Aim 1-3) Develop antibody microarray chips that can be used to measure PTMs associated with glycosylation (GloboH, TF Antigens, AGEs) state or oxidative adducts (nitrotyrosine, 4-HNE, GSH).

Statement of Work Task 1. "Develop antibody microarray chips that can be used to measure PTMs associated with glycosylation (GloboH, TF Antigens, AGEs) state or Oxidation adducts (nTyr, 4-HNE, GSH)". We have successfully developed microarray chips for Globo-H, 4-HNE, and GSH.

Statement of Work Task 4. "Investigate the fundamental biochemistry of the most promising breast cancer biomarkers". As we stated in our original statement of work 4, we further analyzed PTMs within the positive "outcomes". The molecular imaging studies with the chosen PTM antibody (Globo-H) revealed that the translational application of the PTM for non-invasive breast cancer detection.

Difficulties

Identifying protein biomarkers for breast cancer early detection remains a big challenge given the vast range of protein species and broad range concentrations. We intend to develop microarray chips to find whether oxidation and glycosylation modifications can be used for breast cancer detection biomarkers. The big difficulty for this type chip development is hard to find applicable antibodies for the PTM-ELISA.

Discussion for new tracer development for breast cancer early detection

Through the high through-put ELISA microarray assay, we identified several important oxiditive and glycosylation PTMs biomarkers for breast cancer early detection. But the application is limited by the specific antibodies. As the PI of this project has moved to Washington University at St. Louis under the supervision of Dr. Zhude Tu, who has led many years of radiotracer development for breast cancer studies using the PET. This provides the opportunities of developing a specific radiotracer that is able to recognizing these PTM modifications (4-HNE, GSH, Globo-H).

Key Research Accomplishments

1. Validated oxidation modification (GSH, 4HNE) ELISA analysis for breast cancer early detection;
2. Validated glycosylation modification (Globo-H) ELISA analysis for breast cancer early detection;
3. Establish novel glycosylation antibody H6-11 for tumor xenograft mouse;
4. Completed Globo-H antibody microPET imaging studies for MCF-7 tumor xenograft mouse.

Reportable Outcomes

Published Peer Reviewed papers

1. **Jin, H.,** M Xu , PK Padakanti , Y Liu , S Lapi , and Z Tu Preclinical Evaluation of the Novel Monoclonal Antibody H6-11 for Prostate Cancer Imaging, ***Mol. Pharmaceutics***, 2013, Article ASAP, DOI: 10.1021/mp400130w
2. **Jin, H.**, DS Daly JR Marks and RC Zangar Oxidatively modified proteins as plasma biomarkers in breast cancer, ***Cancer Biomarkers***, 2013, 13(3):193-200

Poster

AACR 2013 Abstract #318 Abril 6-10th, 2013 Washington, D.C.
Preclinical Evaluation of Monoclonal Antibody H6-11 for Prostate Cancer Imaging Hongjun Jin, Mai Xu, Prashanth K. Padakanti and Zhude Tu
Department of Radiology Science, Washington University School of Medicine, St. Louis, MO 63110, USA (Appendix)

Patent Approval

Jin, H., and R.C. Zangar, Compositions, Antibodies, Asthma Diagnosis Methods, and Methods for Preparing Antibodies (U.S. 20120094860)

Conclusion

To detect breast cancer in its earlier stages, oxidantion and glycosylation modification PTMs are proposed as potential biomarkers with circulating human proteins. Continued the PTM-ELISA microarray chips (4HNE, GSH and Globo-H), we validated the PTM antibody for molecular imaging for non-invasive breast cancer detection. This work provides a methodological platform for the study of post-translationally-modified proteins. Through this novel PTM-ELISA microarray screening, we found that Globo-H, 4HNE and GSH may be potential useful biomarkers for breast cancer early detection. Some of these antibodies may also be applied for molecular imaging for non-invasive breast cancer early detection.

References

1. Utzon-Frank, N., Vejborg, I., von Euler-Chelpin, M., and Lynge, E. (2011) Balancing sensitivity and specificity: Sixteen year's of experience from the mammography screening programme in Copenhagen, Denmark, *Cancer Epidemiol*.
2. Gotzsche, P. C., and Nielsen, M. (2011) Screening for breast cancer with mammography, *Cochrane Database Syst Rev*, CD001877.
3. Sala, M., Salas, D., Belvis, F., Sanchez, M., Ferrer, J., Ibanez, J., Roman, R., Ferrer, F., Vega, A., Laso, M. S., and Castells, X. (2011) Reduction in false-positive results after introduction of digital mammography: analysis from four population-based breast cancer screening programs in Spain, *Radiology 258*, 388-395.
4. Groenendijk, R. P., Kochen, M. P., van Engelenburg, K. C., Boetes, C., Strobbe, L. J., Ruers, T. J., and Wobbes, T. (2001) Detection of breast cancer after biopsy for false-positive screening mammography. An increased risk?, *Eur J Surg Oncol 27*, 17-20.
5. Aro, A. R., Pilvikki Absetz, S., van Elderen, T. M., van der Ploeg, E., and van der Kamp, L. J. (2000) False-positive findings in mammography screening induces short-term distress - breast cancer-specific concern prevails longer, *Eur J Cancer 36*, 1089-1097.
6. Lidbrink, E., Elfving, J., Frisell, J., and Jonsson, E. (1996) Neglected aspects of false positive findings of mammography in breast cancer screening: analysis of false positive cases from the Stockholm trial, *BMJ 312*, 273-276.
7. Jin, H., and Zangar, R. C. (2009) Protein modifications as potential biomarkers in breast cancer, *Biomarker insights 4*, 191-200.
8. Karihtala, P., Winqvist, R., Syvaoja, J. E., Kinnula, V. L., and Soini, Y. (2006) Increasing oxidative damage and loss of mismatch repair enzymes during breast carcinogenesis, *Eur J Cancer 42*, 2653-2659.
9. Karihtala, P., Kinnula, V. L., and Soini, Y. (2004) Antioxidative response for nitric oxide production in breast carcinoma, *Oncol Rep 12*, 755-759.
10. Yeh, C. C., Hou, M. F., Wu, S. H., Tsai, S. M., Lin, S. K., Hou, L. A., Ma, H., and Tsai, L. Y. (2006) A study of glutathione status in the blood and tissues of patients with breast cancer, *Cell Biochem Funct 24*, 555-559.
11. Perquin, M., Oster, T., Maul, A., Froment, N., Untereiner, M., and Bagrel, D. (2001) The glutathione-related detoxification system is increased in human breast cancer in correlation with clinical and histopathological features, *J Cancer Res Clin Oncol 127*, 368-374.
12. Gromadzinska, J., Wasowicz, W., Andrijewski, M., Sklodowska, M., Quispe, O. Z., Wolkanin, P., Olborski, B., and Pluzanska, A. (1997) Glutathione and glutathione metabolizing enzymes in tissues and blood of breast cancer patients, *Neoplasma 44*, 45-51.

Appendices

Conference Abstracts

AACR Anual Meeting 2013 #318 post session
Abril 6-10th, 2013
Washington, D.C.

Abstract

Preclinical Evaluation of Monoclonal Antibody H6-11 for Prostate Cancer Imaging
Hongjun Jin, Mai Xu, Prashanth K. Padakanti and Zhude Tu
Department of Radiology Science, Washington University School of Medicine, St. Louis, MO 63110, USA
Altered post-translational modification (PTM) of glycosylations to various nuclear and cytosolic proteins is a universal feature of cancer cells and these modified glycan plan significant role in immune surveillance, tumor invasion, and increase malignancy. In this study, we reported a novel monoclonal antibody reacting to the tumor glycoproteins with molecular weight around 40-60 kDa. Deglycosylation examination suggested the antigenic isotope of the glycan is O-linked β-N-acetylglucosamine (O-GlcNAc) group. We examined the reactivity of H6-11 to cancer cells including PC-3, MCF-7 cells and implanted PC-3 and EMT-6 tumor tissues using immunofluorescence staining and autoradiography technique. The Zr-89 labeled H6-11 was successfully synthesized and the microPET study was performed in PC-3 xenograft prostate model in nude mice. microPET study showed that significant amount of radioactivity accumulation was observed in the excretory organs during the early period post-injection of radioactivity. At 24 hrs post-injection of radioactivity, significant amount of radioactivity was observed in the xenograft prostate tumor, while the radioactivity intensity was decreased in the liver and kidney. Radioactivity uptake in the tumor was still evident at 120 hrs post-injection of radioactivity. Our work suggested that the H6-11 antibody is capable of detecting prostate tumors both *in vitro* and *in vivo*.

Cancer Biomarkers 13 (2013) 193–200
DOI 10.3233/CBM-130349
IOS Press

Oxidatively modified proteins as plasma biomarkers in breast cancer

Hongjun Jin[a,b], Don S. Daly[c], Jeffrey R. Marks[d] and Richard C. Zangar[a,*]
[a]*Fundamental and Computational Sciences, Pacific Northwest National Laboratory, Richland, WA, USA*
[b]*Division of Radiological Sciences, Washington University School of Medicine, St. Louis, MO, USA*
[c]*Statistical and Mathematical Sciences, Pacific Northwest National Laboratory, Richland, WA, USA*
[d]*Department of Surgery, Duke University Medical Center, Durham, NC, USA*

Abstract.
BACKGROUND: Post-translational protein modifications (PTMs) are increased in breast tumors.
OBJECTIVE: We explored whether PTMs on proteins secreted by the breast could be detected in plasma and potentially used for the early detection of breast cancer.
METHODS: We used a custom ELISA microarray platform to measure 4-hydroxynonenal (HNE), glutathione (GSH), nitrotyrosine and halotyrosine adducts in 27 secreted proteins, for a total of 108 candidate biomarkers. Two independent sets of human plasma samples were measured, for a total of 160 samples. The results were analyzed for consistent cancer-associated changes across the two sample sets. Plasma samples for both cases and benign controls were collected at the time of tissue diagnosis after referral from a positive screen (such as mammography). The results from both studies were evaluated using ANOVA and t-tests or receiver operator curves (ROC).
RESULTS: Levels of GSH-modified ceruloplasmin and HNE-modified PDGF were significantly altered in plasma samples from cancer patients relative to benign controls. Healthy controls, which were only included in the first set of samples, were similar to the benign controls for both of these markers. A combination of three glutathionylated proteins produced the best area under the ROC curve, with a value of 76%.
CONCLUSIONS: Specific PTMs in individual proteins may be useful for distinguishing between women with breast cancer and those with benign breast disease. These oxidative changes in plasma proteins may reflect redox changes in breast cancer. Additional studies on oxidative modifications in individual proteins are warranted.

Keywords: Breast cancer, biomarkers, reactive oxygen species, protein adducts, hydroxynonenal, glutathione, plasma

1. Introduction

Breast cancer is the second most common cancer and the fifth most common cause of cancer death in the United States. In 2008, breast cancer resulted in 458,000 deaths worldwide according to World Health Organization [1]. Women in the United States have among the highest incidence of breast cancer in the world, with an approximate 1 in 8 lifetime risk of developing breast cancer and a 1 in 35 risk of death. In 2011, there were 230,480 newly diagnosed breast cancer cases in the United States, resulting in 57,650 deaths [2]. The mortality and morbidity associated with breast cancer likely could be reduced by complementary screening method such as circulating biomarkers.

Oxidative stress appears to be a risk factor for breast cancer and may contribute to the pathology of this disease [3]. Oxidative stress is increased in breast cancer [4–6] and the greatest increase is observed during early-stage disease [5]. Oxidative stress is an underlying factor in oxidative modifications of proteins, including proteins that are secreted into the blood. The

*Corresponding author: Richard C. Zangar, Fundamental and Computational Sciences, Pacific Northwest National Laboratory, Richland, P.O. Box 999, WA, USA. E-mail: richard.zangar@pnnl.gov.

ISSN 1574-0153/13/$27.50

primary goal of this study is to determine if oxidatively modified proteins have potential as biomarkers for the early detection of breast cancer regardless of the underlying mechanisms. Even so, oxidatively modified tumor proteins that are detected in blood could provide insight into molecular processes occurring in the tumor. Reactive oxygen species (ROS), which are responsible for oxidative protein modifications, regulate important processes in epithelial cancers such as activation of MAPK/Erk and PI3K/Akt pathways [7]. In cultured human mammary epithelial cells, we found that both of these signaling pathways and intracellular ROS regulate the secretion of a variety of autocrine factors, paracrine factors and matrix metalloproteases [8,9]. Based on these studies, we hypothesized that alterations in cell signaling and oxidative stress associated with breast cancer would not only result in increased levels of certain proteins that are secreted into blood but that these proteins would have unusually high oxidation rates. As such, these oxidized proteins could serve as circulating breast cancer biomarkers.

In this study, we evaluate oxidative, post-translational protein modifications (PTMs) that are potentially characteristic of early breast cancer. Because we expect the modified proteins to be at low abundance, we use the sandwich enzyme-linked immunosorbent assays (ELISAs) because these assays have exceptional sensitivity and specificity. In the sandwich ELISA, one antibody is used to capture and concentrate the target protein and a second antibody selectively measures the oxidative modification. Although neither the individual proteins nor the modification may be unique to breast cancer, we hypothesized that an increase of both secretory and oxidative processes in breast cancer tissue would result in useful biomarkers. Our results suggest that oxidatively modified proteins are altered in plasma from breast cancer patients and that these proteins have potential to be used as biomarkers for this disease.

2. Materials and methods

2.1. Human subjects

All subjects were recruited and samples were collected under Institutional Review Board (IRB)-approved protocols and informed consent at the Duke University. The Duke IRB protocols were subsequently reviewed and approved by the IRB at the Pacific Northwest National Laboratory prior to transfer and analysis of the samples. Two sets of plasma samples were analyzed for a total of 160 subjects. The first sample set contained plasma from 22 subjects with benign breast disease tumors, 24 subjects with invasive breast cancer and 22 healthy controls (total of 68 subjects). The second sample set contained plasma from 54 subjects with benign breast disease and 38 with invasive breast cancer (total of 92 subjects).

Table 1
Subjects characteristics

	Healthy controls	Benign controls	Invasive cancer	Total
Sample set 1				
N	22	22	24	68
Age (years)	46 ± 16[a]	52 ± 14	50 ± 8	50 ± 13
Race (B/H/W[b])	6/1/15	6/0/16	3/0/21	15/1/52
BMI (kg/m^2)	23 ± 1	26 ± 3	26 ± 4	26 ± 4
Sample set 2				
N	0	54	38	92
Age (years)	NA	53 ± 13	53 ± 11	53 ± 12
Race (B/H/W)	NA	0/0/54	0/0/38	0/0/92
BMI (kg/m^2)	NA	26 ± 5	30 ± 8	28 ± 7

[a]Mean ± SE.
[b]Abbreviations: B, Black; H, Hispanic; W, White; BMI, Body Mass Index. NA, Not applicable.

All plasma samples were collected in the same clinical setting, using the same protocol. All subjects had received a positive screen (e.g., mammography) and were therefore referred for an image-guided biopsy, at which time the blood samples were collected. Since it was unknown until after the pathological analysis which subjects had breast cancer and which had benign disease, this study design minimizes the possibility of potentially confounding factors such as behavioral changes or emotional stress associated with knowledge of cancer by the subjects. Samples in the control groups were selected to correspond to the cancer cases based on the subject's age, body mass index (BMI), and race (Table 1).

2.2. Processing of plasma samples

Plasma samples were stored as individual aliquots at −80°C until use. Immediately before analysis, the samples were thawed on ice and centrifuged at 15,000 g for 20 min at 4°C to remove trace precipitates. The supernatant was diluted 5-fold in 0.1% BSA/PBS containing 1000 pg/mL of green fluorescent protein, which was used as the antigen in a calibrant sandwich ELISA to identify and normalize any chip-to-chip bias [10,11]. The individual capture antibodies (listed in Supplementary Table 1) are typically saturated by low ng/mL concentrations of antigen, and we

routinely dilute plasma samples 500-fold in order to get antigen concentrations in the usable range of the standard curve for the unmodified proteins. We previously demonstrated that capture antibodies for the plasma proteins are typically saturated at a 5-fold dilution of plasma [12]. As such, the 5-fold dilution of plasma used in this study is expected to saturate the capture antibodies, resulting in approximately equal masses of captured antigen on each spot. Thus, the PTM signal should be relative to a consistent mass of antigen and not be influenced by plasma variations in antigen concentrations.

2.3. ELISA microarray analysis

The basic ELISA microarray protocol has been previously described in detail [13]. In brief, 27 capture antibodies (listed in supplementary Table 1) were printed on each chip in quadruplicate spots such that one replicate spot per antibody was printed in each of 4 identical quadrants (Fig. 1). The commercial sources for these antibodies have been previously reported [12,14]. A capture antibody for the green fluorescent protein, which was used as a sandwich ELISA calibration assay (see below), and orientation spots were also printed in quadruplicate on each chip (Fig. 1). The samples were blocked based on study group and then randomized for the ELISA analysis. The 4 PTM analyses were each conducted separately. Individual chips were first incubated with a diluted plasma sample from a single subject, with each sample analyzed on 3 identical chips for each of the 4 PTM analyses. Thus, this study represents data from 1920 ELISA chips and 51,840 ELISAs, without taking into account the 4 replicate spots for each assay on each chip. For each PTM analysis, all samples were simultaneously processed, thus eliminating concerns about reagent drift or other potential day-to-day variations. After washing, the chips were incubated with one of 4 biotinylated PTM detection antibodies (listed in supplementary Table 2) and a biotinylated detection antibody for green fluorescent protein. The biotin signal was amplified using the biotinyltyramide system [15]. Fluorescent labeling was produced using streptavidin conjugated with Alexa 546. After processing, the microarray slides were imaged with a fluorescent laser scanner (ScanArray Express HT, Perkin-Elmer, Downer Grove, IL, USA) and ScanArray Express software was used to quantify the fluorescent intensity of the spots. Data calibration across chips was undertaken using the data from the green fluorescent protein ELISA analysis using ProMAT Calibrator [10,11] and then was processed using ProMAT [16]. We developed both of these programs as open-source programs in R that are freely available on the web (www.pnl.gov/statistics/ProMAT/).

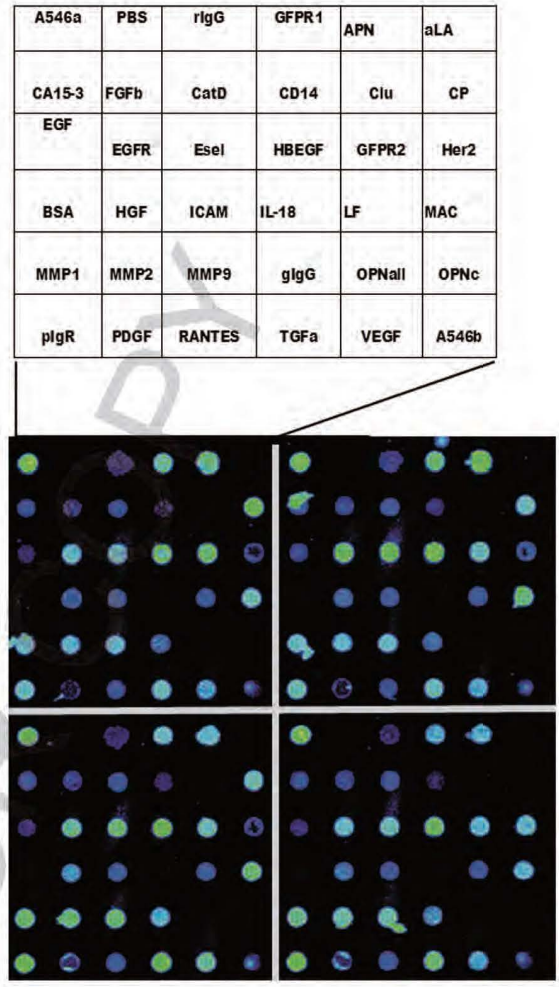

Fig. 1. Image of a single ELISA microarray. Each microarray chip contains 27 capture antibodies for assay proteins and additional control spots for orientation (A546) and antibodies for an internal calibration assay (GFP). All reagents were individually printed in quadruplicate (once in each quadrant). A single scanned chip is shown in the lower image, with crossed white lines added to seperate the 4 identical quadrants. The color is artificial and corresponds to fluorescence signal intensity, which increases from black (background) to blue (weak fluorescent signal) to green (strong signal). The layout of a single quadrant is shown in the upper figure. (Colours are visible in the online version of the article; http://dx.doi.org/10.3233/CBM-130349)

2.4. Statistics

Results from within and across reagents and studies were statistically evaluated, individually and in combination, using ANOVA, t-tests and ROC analyses. First,

Table 2
Summary of t-test results for GSH and HNE oxidative modification on 26 individual proteins for data from two independent sets of plasma samples. No significant changes were observed for nitrotyyrosine and halotyrosine P values < 0.05 are highlighted

	First study		Second study		Both
Assay	Benign Signal	Cancer Signal	Benign Signal	Cancer Signal	t-test p value
GSH-aLB	10153	10808	1277	1174	0.67
GSH-APN	3827	4190	1582	2250	0.70
GSH-CA15-3	5831	5565	478	168	0.49
GSH-CatD	3497	2831	901	1370	0.56
GSH-CD14	4236	3283	1000	569	0.26
GSH-Clu	1701	2722	723	1265	0.11
GSH-CP	4960	5988	392	442	**0.004**
GSH-E-Selectin	834	850	880	1234	0.69
GSH-EGF	4965	3604	376	400	0.31
GSH-EGFR	457	390	690	981	0.82
GSH-bFGF	6747	7062	1021	834	0.56
GSH-HBEGF	1660	1598	1293	1504	0.89
GSH-Her2	1757	1585	438	369	0.70
GSH-HGF	3133	1654	783	661	**0.02**
GSH-ICAM	1900	1567	1375	863	0.73
GSH-IL-18	98	85	1111	1113	0.11
GSH-Lfn	11040	9062	352	311	0.27
GSH-MAC-2BP	299	210	303	392	0.65
GSH-MMP1	348	291	320	542	0.96
GSH-MMP2	257	188	266	390	0.37
GSH-MMP9	328	261	659	1214	0.46
GSH-OPN	105	122	697	660	0.57
GSH-PDGF	2065	1680	1459	1166	0.78
GSH-pIgR	344	323	607	1017	0.83
GSH-RANTES	377	433	2504	1738	0.90
GSH-TGFa	323	235	715	830	0.42
GSH-VEGF	143	104	243	296	0.18
HNE-aLB	77	99	1739	1749	0.49
HNE-APN	476	424	535	570	0.93
HNE-CA15-3	568	553	2745	2371	0.39
HNE-CatD	656	641	634	599	0.89
HNE-CD14	1042	900	452	440	0.88
HNE-Clu	77	94	339	348	0.34
HNE-CP	632	616	267	275	0.37
HNE-E-selectin	1893	627	1267	1385	0.78
HNE-EGF	796	691	26673	25932	0.23
HNE-EGFR	1233	259	695	726	0.09
HNE-bFGF	231	1510	681	742	0.09
HNE-HB-EGF	2506	1133	864	899	0.46
HNE-Her2	855	799	1151	1127	0.96
HNE-HGF	2969	2348	932	699	0.18
HNE-ICAM	1069	879	1717	1421	0.40
HNE-IL-18	96	126	1353	1080	0.05
HNE-Lfn	2814	2380	2289	1845	0.18
HNE-MAC-2BP	3283	2024	806	764	0.32
HNE-MMP1	1212	216	711	713	0.05
HNE-MMP2	1232	198	724	644	**0.039**
HNE-MMP9	1034	244	618	690	0.23
HNE-OPN	86	105	352	411	0.18
HNE-PDGF	777	558	2063	1723	**0.0013**
HNE-pIgR	1693	326	799	794	**0.009**
HNE-RANTES	466	306	760	657	0.84
HNE-TGFa	1114	174	856	726	0.08
HNE-VEGF	752	145	642	579	0.17

promising reagent-specific assays were identified by using Box-Cox transformed ELISA spot-fluorescence data and then comparing individual assays between the cancer and no-cancer groups by ANOVA. The ANOVA model included a two-level study factor to account for intensity offsets between studies while the intensities were Box-Cox transformed in order to produce normally distributed residuals of the same scale between studies. When P was less than 0.05 for the ANOVA analysis, statistical differences between individual groups were delineated by t-tests. In these cases, only the t-test p values are presented here. Assay results were then evaluated with ROC analyses of the individual assays and linear discriminant scores of assay combinations. ROC curves were computed using data from the two individual studies and the data combined across studies using the Moses algorithm [17]. These analyses were executed using R [18] with Box-Cox transform and linear discriminant algorithms from the MASS [19] library, and ROC algorithms from the ROCR library [20].

3. Results

3.1. GSH and HNE modifications in plasma proteins are altered in breast cancer

We analyzed 4 PTMs in 27 proteins for an analysis of 108 total candidate biomarkers. We used several criteria to identify likely candidate proteins for our analysis. First, we selected potential biomarkers based on our proteomics study that identify abundant proteins in nipple aspirate fluid, which is highly enriched in proteins secreted by the breast ductal tissue, the cells of which are the source of most breast cancers [21]. We also analyzed a number of secreted proteins reported by others to be produced by normal or cancerous breast tissue. Finally, we evaluated a selection of proteins that we identified as being secreted at higher levels in human mammary cells in response to modest changes in intracellular ROS or to epidermal-growth-factor signaling [8,9,22,23].

No differences were observed for halotyrosine or nitrotyrosine protein modifications across the two groups. Although we anticipated that oxidative protein adducts would be increased in breast cancer patients, only glutathione adducts to ceruloplasmin were found at higher levels in the breast-cancer subjects compared to benign controls in both sets of samples (Fig. 2 and Table 2). In contrast, GSH adducts to hep-

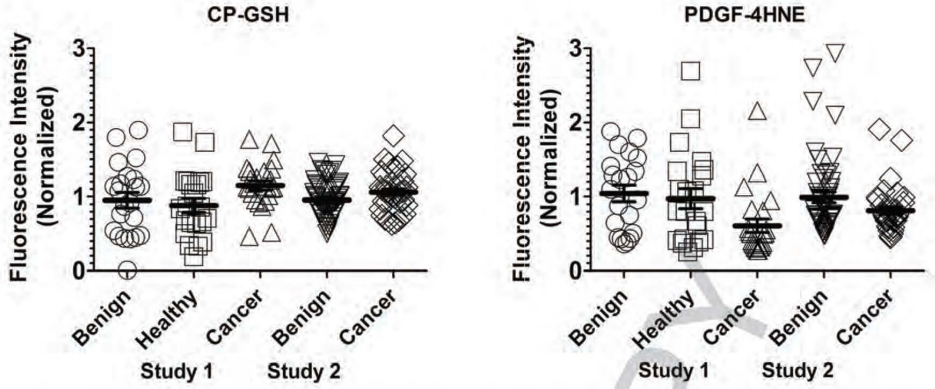

Fig. 2. Representative graphs of normalized fluorescence data for oxidative modifications in individual proteins found in plasma. Data are shown for two independent sets of plasma samples (Study 1 and 2). Each datapoint represents the average raw fluorescence signal for triplicate analyses (one chip per analysis) of a single sample. Since the fluorescent values are in arbitrary units, the data was normalized based on the average value of all the assays for each of the two studies. Data values for each assay on each individual chip were calculated as the median value of 4 identical assay spots. Thus, each datapoint shown here represents data derived from 12 analyses. The central horizontal bar and cross bars represent the mean and the standard error, respectively. CP-GSH, glutathionylated ceruloplasmin; PDGF-4HNE, 4-hydroxynonenal-adducted platelet-derived growth factor.

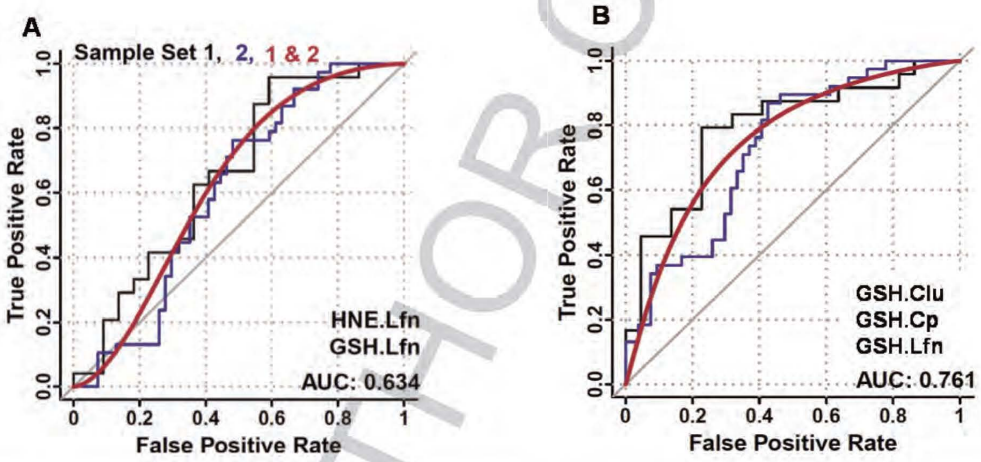

Fig. 3. The best ROC curves for plasma biomarkers on a single protein with different modifications or for a single modification on different proteins. Graphs represent comparisons between oxidatively modified protein levels, as measured in plasma, with comparisons between subjects with invasive breast cancer and those with benign breast disease. A. The combination of three different PTMs biomarkers: 4-hydroxynonenal (HNE) and glutathione (GSH) adducts on lactoferrin (Lfn) produced an area under the fitted ROC curve (AUC) of 63%. B. The combination of ceruloplasmin (Cp), lactoferrin (Lfn) and clusterin (Clu) modified with glutathione adducts (GSH) produced an AUC of 76%. The black and the blue lines represent the empirical data for the first and second sample sets, respectively, and the red line is a fitted curve derived from both sample sets. (Colours are visible in the online version of the article; http://dx.doi.org/10.3233/CBM-130349)

atocyte growth factor were lower in the breast cancer subjects relative to the benign controls. We and others previously found that levels of circulating hepatocyte growth factor are increased in recurrent breast cancer patients relative to healthy controls [15,24], suggesting that the decrease in oxidatively modified hepatocyte growth factor is not influenced by a decrease in total levels of this protein.

The levels of three HNE-adducted proteins (i.e., matrix metalloprotease 2, platelet-derived growth factor A [PDGF] and polyimmunoglobin receptor) were significantly lower in breast cancer patients compared to the benign controls (Table 2). PDGF-HNE, which had the greatest difference between the two groups, is shown in Fig. 2.

3.2. *Alterations in PTM combinations between breast cancer and healthy controls*

For this comparison, we focused on differences between women with invasive cancer and those with no

breast abnormality as determined by screening mammography. Results from the multiple PTM-modified proteins were combined using ROC analyses. For this analysis, we focused on either multiple proteins with the same PTM or on different PTMs found on a single protein. That is, we did not evaluate all possible combinations of PTMs across all proteins. The combination of three different proteins, ceruloplasmin, hepatocyte growth factor and clusterin, all with GSH adducts, produced an area under the ROC curve (AUC) of 76% (Fig. 3) when data from the two studies was combined. This result was the best observed for any three proteins with the same oxidative modification. In addition, the combination of lactoferrin with either GSH or HNE modifications had an AUC value of 0.63 (Fig. 3). This result was the best observed for any single protein with more than one oxidative modification.

4. Discussion

Cancer has been compared to "a wound that never heals", implying that chronic oxidative stress from inflammation is important in cancer development. In addition, other cancer-related processes can increase ROS in breast tumors, potentially altering gene expression and cellular function [25,26]. The levels of individual PTMs are broadly increased in breast cancer tissue [4]. To determine if a specific protein modification could be a useful biomarker, we examined single oxidative modifications on individual proteins that are secreted by the breast. Because there is insufficient knowledge to predict which PTMs are likely to be most useful, we examined 108 combinations of oxidative protein modifications (4 modifications on each of 27 different proteins).

One oxidative modification we evaluated was HNE, which is a nonenzymatic byproduct of lipid peroxidation that spontaneously adducts to proteins. Protein-bound HNE in the tumor tissue is increased in more than one stage of breast cancer, but HNE levels are highest in early breast cancer relative to the adjacent tissue [5,27] suggesting that HNE modifications may be particularly useful for detecting early-stage disease. Surprisingly, three proteins had changes in the levels of HNE adducts and in all cases HNE adducts were suppressed in the blood of breast cancer patients relative to benign controls. The meaning of this change remains uncertain and could relate to either decreased formation of these adducts or an increase in their plasma clearance in breast cancer patients.

In vitro, lipid peroxidation and the associated HNE adducts result from relatively severe oxidative stress that occurs when the cellular antioxidant defense system is overwhelmed. More subtle changes in the intracellular redox environment likely precede severe oxidative stress. Cysteine is the most readily oxidized amino acid and susceptible cysteine residues are oxidized under physiological redox conditions and are converted to GSH-cysteine protein adducts. We therefore examined GSH adducts as an indicator of subtle changes in redox status. Modest redox changes may contribute to breast cancer development and progression by altering intracellular signaling and cell-to-cell communication. For example, we found that modest increases in intracellular ROS production altered the expression and secretion of a variety of bioactive proteins in several epithelial cell lines [9]. This prior study found that in human mammary cells, expression of low-levels of a ROS-generating protein increased secretion of TGFα, a ligand for the epidermal growth factor receptor, but suppressed secretion of matrix metalloprotease 1. The general effects of ROS on protein secretion were conserved across epithelial cells from different tissues and mammalian species, but the individual secreted proteins varied with cell type.

We examined protein halotyrosine modifications, which are primarily the result of granulocyte peroxidase activities [28]. In a previous analysis of proteins in sputum, we found elevated levels of halogenated proteins in asthma patients with either eosinophilic or neutrophilic disease relative to healthy controls (unpublished data). However, there is a lack of evidence for a role for these granulocytes in breast cancer development. As such, we included the halotyrosine analysis as a type of negative control assay, anticipating that this protein modification would not be associated with breast cancer. As we did not observe any changes in protein halogenation, our results provide additional evidence that these granulocytes are not associated with breast cancer.

Similar to halotyrosine, we found that protein nitrotyrosine levels were not significantly different between cancer patients and either benign or healthy controls. This relationship was not anticipated because nitrotyrosine modifications are commonly associated with many different human diseases, including breast cancer [29]. In breast tumors, increases in protein nitrotyrosine are found in the vicinity of infiltrating inflammatory cells [30]. We previously analyzed nitrotyrosine levels in individual proteins found in plasma from 458 subjects. This study found that nitrotyrosine levels were associated with chronic obstructive pulmonary disease and tobacco smoke exposure, suggesting that the nitration of plasma proteins is influenced both by inflammation and endothelial nitric oxide synthase activity, which appears to be suppressed

by smoking [12]. These results suggest that multiple processes influence nitration levels of plasma proteins and that these processes may mask any cancer-related nitration changes in the proteins we analyzed.

Overall, the general markers of oxidative stress and changes in redox status, HNE, and GSH proved to be more promising cancer biomarkers than nitrotyrosine or halotyrosine. These latter two processes are more likely to be indicators of specific inflammatory processes while the first two processes are non-specific markers of changes in oxidative stress and redox status. Our most promising results were observed when data from several oxidatively modified proteins were combined, a result that is consistent with our prior analysis of unmodified proteins as breast cancer biomarkers [31]. Further studies are needed to replicate and confirm the results reported here.

Acknowledgements

This research was supported by NIH U01 CA117378 (RCZ), NIH UO1 CA084955 (JRM), and a US Department of Defense BCRP Postdoctoral Fellowship W81XWH-10-1-0031 (HJ).

References

[1] World Health Organization. Fact Sheet. 2008. http://www.who.int/mediacentre/factsheets/fs297/en/.
[2] R. Siegel, D. Naishadham, and A. Jemal. Cancer statistics, 2012. CA Cancer J Clin **62** (2012); 10-29.
[3] C.B. Ambrosone. Oxidants and antioxidants in breast cancer. Antioxid Redox Signal **2** (2000); 903-917.
[4] H. Jin and R.C. Zangar. Protein modifications as potential biomarkers in breast cancer. Biomark Insights **4** (2009); 191-200.
[5] P. Karihtala, R. Winqvist, J.E. Syvaoja, V.L. Kinnula, and Y. Soini. Increasing oxidative damage and loss of mismatch repair enzymes during breast carcinogenesis. Eur J Cancer **42** (2006); 2653-2659.
[6] J. Marx. Cancer research. Inflammation and cancer: the link grows stronger. Science **306** (2004); 966-968.
[7] W.S. Wu. The signaling mechanism of ROS in tumor progression. Cancer Metastasis Rev **25** (2006); 695-705.
[8] R.C. Zangar, N. Bollinger, T.J. Weber, R.M. Tan, L.M. Markillie, and N.J. Karin. Reactive oxygen species alter autocrine and paracrine signaling. Free Radic Biol Med **51** (2011); 2041-2047.
[9] Y. Zhang, R.M. Gonzalez, and R.C. Zangar. Protein secretion in human mammary epithelial cells following HER1 receptor activation: influence of HER2 and HER3 expression. BMC Cancer **11** (2011); 69.
[10] D.S. Daly, K.K. Anderson, S.L. Seurynck-Servoss, R.M. Gonzalez, A.M. White, and R.C. Zangar. An internal calibration method for protein-array studies. Stat Appl Genet Mol Biol **9** (2010); Article.
[11] R.C. Zangar, D.S. Daly, A.M. White, S.L. Servoss, R.M. Tan, and J.R. Collett. ProMAT calibrator: A tool for reducing experimental bias in antibody microarrays. J Proteome Res **8** (2009); 3937-3943.
[12] H. Jin, B.J. Webb-Robertson, H. Petersen, R.M. Tan, D. Bigelow, M.B. Scholand, J.R. Hoidal, J.G. Pounds, and R.C. Zangar. Smoking, COPD and nitrotyrosine levels of plasma proteins. Environ Health Perspect **119** (2011); 1314-1320.
[13] H. Jin and R.C. Zangar. High-throughput, multiplexed analysis of 3-nitrotyrosine in individual proteins. Curr Protoc Toxicol **Chapter 17** (2012).
[14] R.M. Gonzalez, S.L. Seurynck-Servoss, S.A. Crowley, M. Brown, G.S. Omenn, D.F. Hayes, and R.C. Zangar. Development and validation of sandwich ELISA microarrays with minimal assay interference. J Proteome Res **7** (2008); 2406-2414.
[15] R.L. Woodbury, S.M. Varnum, and R.C. Zangar. Elevated HGF levels in sera from breast cancer patients detected using a protein microarray ELISA. **2003/03/21** (2002); 233-237.
[16] A.M. White, D.S. Daly, S.M. Varnum, K.K. Anderson, N. Bollinger, and R.C. Zangar. ProMAT: protein microarray analysis tool. **2006/04/06** (2006); 1278-1279.
[17] L.E. Moses, D. Shapiro, and B. Littenberg. Combining independent studies of a diagnostic test into a summary ROC curve: data-analytic approaches and some additional considerations. Stat Med **12** (1993); 1293-1316.
[18] R Development Team. A language and environment for statistical computing. In: R Foundation for Statistical Computing, editor. 2010.
[19] W.N. Venables, and B.D. Ripley. Modern Applied Statistics with S. 4th ed. Springer; 2002.
[20] T. Sing, O. Sander, N. Beerenwinkel, and T. Lengauer. ROCR: visualizing classifier performance in R. Bioinformatics **21** (2005); 3940-3941.
[21] S.M. Varnum, C.C. Covington, R.L. Woodbury, K. Petritis, L.J. Kangas, M.S. Abdullah, J.G. Pounds, R.D. Smith, and R.C. Zangar. Proteomic characterization of nipple aspirate fluid: identification of potential biomarkers of breast cancer. Breast Cancer Research and Treatment **80** (2003); 87-97.
[22] W.N. Chen, R.L. Woodbury, L.E. Kathmann, L.K. Opresko, R.C. Zangar, H.S. Wiley, and B.D. Thrall. Induced autocrine signaling through the epidermal growth factor receptor contributes to the response of mammary epithelial cells to tumor necrosis factor alpha. J Biol Chem **279** (4-30-2004); 18488-18496.
[23] K.D. Rodland, N. Bollinger, D. Ippolito, L.K. Opresko, R.J. Coffey, R. Zangar, and H.S. Wiley. Multiple mechanisms are responsible for transactivation of the epidermal growth factor receptor in mammary epithelial cells. J Biol Chem **283** (2008); 31477-31487.
[24] M. Maemura, Y. Iino, T. Yokoe, J. Horiguchi, H. Takei, Y. Koibuchi, Y. Horii, I. Takeyoshi, S. Ohwada, and Y. Morishita. Serum concentration of hepatocyte growth factor in patients with metastatic breast cancer. Cancer Lett **126** (4-24-1998); 215-220.
[25] D.R. Gough, and T.G. Cotter. Hydrogen peroxide: a Jekyll and Hyde signalling molecule. Cell Death Dis **2** (2011); e213.
[26] H. Antelmann, and J.D. Helmann. Thiol-based redox switches and gene regulation. Antioxid Redox Signal **14** (3-15-2011); 1049-1063.
[27] P. Karihtala, S. Kauppila, U. Puistola, and A. Jukkola-Vuorinen. Divergent behaviour of oxidative stress markers 8-hydroxydeoxyguanosine (8-OHdG) and 4-hydroxy-2-nonenal (HNE) in breast carcinogenesis. Histopathology **58** (2011); 854-862.

[28] W. Wu, M.K. Samoszuk, S.A. Comhair, M.J. Thomassen, C.F. Farver, R.A. Dweik, M.S. Kavuru, S.C. Erzurum, and S.L. Hazen. Eosinophils generate brominating oxidants in allergen-induced asthma. J Clin Invest **105** (2000); 1455-1463.
[29] P. Karihtala, V.L. Kinnula, and Y. Soini. Antioxidative response for nitric oxide production in breast carcinoma. Oncol Rep **12** (2004); 755-759.
[30] M. Samoszu, M.L. Brennan, V. To, L. Leonor, L. Zheng, X. Fu, and S.L. Hazen. Association between nitrotyrosine levels and microvascular density in human breast cancer. Breast Cancer Res Treat **74** (2002); 271-278.
[31] R.M. Gonzalez, D.S. Daly, R. Tan, J.R. Marks, and R.C. Zangar. Plasma biomarkers profiles differ depending on breast cancer subtype but RANTES is consistently increased. Cancer Epidemiol Biomarkers Prev **20** (2011); 1543-1551.

Supplementary materials

Oxidatively modified proteins as candidate biomarkers in breast cancer

Hongjun Jin[1], Don Daly[2], Jeffrey R. Marks[3] and Richard Zangar[1]

[1]*Cell Biology and Biochemistry, Fundamental and Computational Sciences Directory, Pacific Northwest National Laboratory, Richland, WA, USA*
[2]*Statistical and Mathematical Sciences, Pacific Northwest National Laboratory, Richland, WA, USA*
[3]*Duke University Medical Center, Department of Sur- gery, Durham, NC, USA*

Table 1: Capture antibodies for ELISA microarray

Antigen	Antibody source and catalog number
α-lactalbumin	R&D Systems MAB262
Aminopetidase *N*	R&D Systems AF3815
Basic fibroblast growth factor	R&D Systems MAB233
Cancer antigen 15-3	Fitzgerald Industries M81071022
CD14	R&D Systems MAB3833
Cathepsin D	R&D Systems AF1014
Clusterin	R&D Systems AF2937
Ceruloplasmin	Santa Cruz sc-69767
Epidermal growth factor (EGF)	R&D Systems DY236 kit
EGF receptor (extracellular domain)	R&D Systems AF231
E-selectin	R&D Systems AF724
Intracellular adhesion molecular 1	R&D Systems MAB720
Interleukin 18	Medical and Biological Labs D044-3
Her2 (extracellular domain)	NeoMarkers MS-229
Heparin-binding epidermal growth factor	R&D Systems AF292
Hepatocyte growth factor	R&D Systems MAB694
Lactoferrin	Santa Cruz sc-52048
Matrix metalloproteases 1	R&D Systems AF901
Matrix metalloproteases 2	R&D Systems AF902
Matrix metalloproteases 9	R&D Systems AF911
MAC-2 binding protein	R&D Systems AF2226
Osteopontin	R&D Systems MAB14332
Polyimmunoglobin receptor	R&D Systems AF2717
Platelet-derived growth factor AA	R&D Systems MAB221
RANTES (CCL5)	R&D Systems MAB678
Transforming growth factor alpha	R&D Systems AF239
Vascular endothelial growth factor	R&D Systems AF293

Table 2: Detection antibodies used in the ELISA microarrays. These antibodies were used to detect a single oxidative modification, independent of the adjacent sequence, on the proteins listed in Supplementary Table 1

Antigen	Antibody source
Nitrotyrosine	Hycult biotechnology[i]
Glutathione (GSH)	Virogen[ii]
Hydroxynonenal (HNE)	OXIS international[iii]
Halotyrosine	Custom mAb by Zangar Lab (Available from Santa Cruz[iv])

[i]Hycult Biotech Inc., 600 West Germantown Pike, Suite 110, Plymouth Meeting, PA 19462 USA.
[ii]ViroGen Corporation, 200 Dexter Avenue, Watertown, MA 02472 USA.
[iii]OXIS International, U.S. Headquarters, 468 N. Camden Dr., 2nd Floor, Beverly Hills, CA 90210 USA.
[iv]Santa Cruz Biotechnology, Inc., 10410 Finnell Street, Dallas, Texas 75220 USA.

molecular pharmaceutics

Article

pubs.acs.org/molecularpharmaceutics

Preclinical Evaluation of the Novel Monoclonal Antibody H6-11 for Prostate Cancer Imaging

Hongjun Jin, Mai Xu, Prashanth K. Padakanti, Yongjian Liu, Suzanne Lapi, and Zhude Tu*

Department of Radiology, Washington University School of Medicine, 510 S. Kingshighway Boulevard, St. Louis, Missouri 63110, United States

Supporting Information

ABSTRACT: The biological properties of the novel monoclonal antibody (mAb) H6-11 and its potential utility for oncological imaging studies were evaluated using *in vitro* and *in vivo* assays. Immunoreactivity of H6-11 to the human prostate cancer PC-3 cell line and solid tumor xenografts was initially demonstrated using immunofluorescence staining; the specificity of H6-11 for prostate cancer was further evaluated using a commercial array of human prostate cancer and normal tissue samples (n = 49) in which H6-11 detected 95% of prostate adenocarcinomas. The K_d value of 61.7 ± 30 nM was determined using ^{125}I-labeled H6-11. Glycosylation analysis suggested the antigenic epitope of the glycan is an O-linked β-*N*-acetylglucoside (*O*-GlcNAc) group. Imaging studies of PC-3 tumor-bearing mice were performed using both optical imaging with NIR fluorescent dye-labeled H6-11 and microPET imaging with ^{89}Zr-labeled H6-11. These *in vivo* studies revealed that the labeled probes accumulated in PC-3 tumors 48−72 h postinjection, although significant retention in liver was also observed. By 120 h postinjection, the tumors were still evident, although the liver showed significant clearance. These studies suggest that the mAb H6-11 may be a useful tool to detect prostate cancer *in vitro* and *in vivo*.

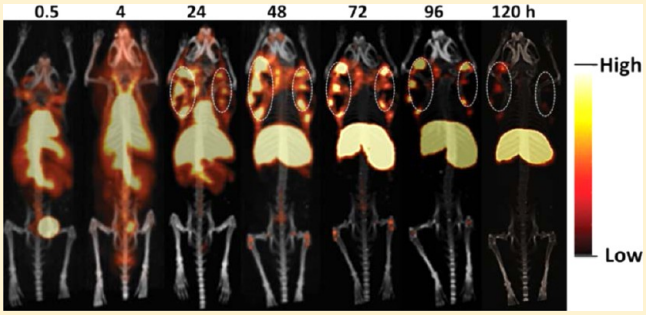

KEYWORDS: *prostate cancer, mAb, O-GlcNAc, positron emission tomography (PET), PC-3, glycosylation, tumor-associated carbohydrate antigens (TACA)*

INTRODUCTION

Cancer cells can demonstrate unusual patterns of glycosylation which result in high levels of specific tumor-associated carbohydrate antigens (TACA). There is considerable evidence that some of these residues are associated with breast cancer,[1,2] prostate cancer,[3−7] and other cancers.[8−10] Several carbohydrate antigens, including the TF and Tn antigens,[3,11,12] sialyl Lewis^X,[4,13] and Globo-H[14−16] have been reported to be important in cancer development and progression. These structural changes can alter cellular function including a cancer cell's adhesive properties and potential to invade and metastasize. A growing body of evidence indicates that proteins synthesized by early stage tumors are subject to post-translational modifications including altered glycosylation pathways which have been associated with immune response.[9,10,17,18] Because glycosylation of cancer-related biomarkers can be determined using specific antibodies, we hypothesized that antibodies against specific glycosylation would be valuable tools for *in vivo* cancer detection.

The potential utility of circulating glycoprotein markers such as CA-125 and human epididymis protein (HE)4 to identify and monitor the progression of prostate and other cancers have been extensively investigated in the clinic.[8,19] Such markers have been particularly useful in monitoring therapeutic response and for detecting tumor recurrence post-treatment. Although studies have revealed that CA-125 is not tumor specific,[20,21] the strategy of combining multiple tumor markers found in serum has been shown to facilitate the detection of early stage tumors and accurately identify tumor recurrence.[22,23] Unfortunately, serum markers cannot be used to determine tumor volume or location, which is critical information in the clinical management of cancer patients. Antibodies which recognize glycoprotein markers have been used for preclincal positron emission tomography (PET) studies as well as clinical studies with single photon emission computed tomography (SPECT) probes and show selective binding to tumors over healthy tissues.[24−26] In the current study, the novel mAb H6-11 originally identified using the human colon adenocarcinoma cell line, NSY42129,[27] was evaluated against a panel of 40 human prostate carcinoma samples, 8 samples of normal prostate tissue, and 1 hepatic carcinoma sample; the expression of mAb H6-11 binding epitope in the PC-3 prostate cancer cell line was also examined. We found that mAb H6-11 recognizes a β-*N*-acetylglucoside group. We further explored the feasibility of imaging solid

Received: March 5, 2013
Revised: August 6, 2013
Accepted: August 21, 2013

tumor xenografts of PC-3 in athymic nu/nu mice by optical imaging and microPET. In these studies, mAb H6-11 distinguished the tumor from surrounding normal tissue. Thus, a glycoprotein-recognizing antibody like mAb H6-11 may be valuable for prostate cancer imaging.

EXPERIMENTAL SECTION

Cell Lines and Cell Culture. Human colon adenoma cell line NSY42129 was cultured in RPMI 1640 supplemented with 10% fetal calf serum (FCS) (Hyclone Laboratory Inc., Logan, Utah), 50 units/mL sodium penicillin (BioWhittaker Inc., Walkersville, Maryland), and 50 μg/mL streptomycin sulfate (BioWhittaker). Myeloma cells (P3/x63·Ag8) used as a fusion partner were maintained in Iscove's modified Dulbecco's medium supplemented with 20% fetal bovine serum (FBS) (Hyclone), 50 units/mL sodium penicillin, 50 μg/mL streptomycin sulfate, 4 mmol/L L-glutamine (BioWhittaker), 1 mM sodium pyruvate (BioWhittaker), and 0.0001% β-mercaptoethanol (Sigma-Aldrich Inc., St. Louis, MO). The human prostate cancer PC-3 cell line was cultured in RPMI 1640 medium supplemented with 10% FCS, 50 units/mL sodium penicillin, 50 units/mL streptomycin sulfate, and 2 mM L-glutamine. MCF-7 human breast cancer cells were maintained in DMEM supplemented with 10% FCS, 50 units/mL sodium penicillin, and 50 units/mL streptomycin sulfate. H6-11 hybridoma cells used for antibody production (H-20, obtained through the Washington University School of Medicine Hybridoma Center) were cultured in Iscove's modified Dulbecco's medium supplemented with 20% fetal bovine serum, 50 units/mL sodium penicillin, 50 units/mL streptomycin sulfate, 4 mM L-glutamine, 1 mM sodium pyruvate, and 0.0001% β-mercaptoethanol. All cells were cultured in a humidified incubator at 37 °C with 5% CO_2. For cDNA sequencing, the frozen H6-11 hybridoma cell line was sent to GenScript Inc. (Piscataway, New Jersey). The consensus complementarity-determining regions (CDR) DNA sequencing was successfully achieved through 10 codon RT-PCR following standard procedures.

Generation of mAb H6-11. All animal procedures were performed according to protocols approved by the Animal Studies Committee of the Washington University School of Medicine in accordance with the Guide for the Care and Use of Laboratory Animals. As previously described,[9,18] 6-week-old female BALB/c mice were injected i.p. with Titermax Gold adjuvant (25 μL; Sigma-Aldrich) and NSY42129 cells (1×10^6) once a week for 4 weeks. Three days before euthanasia, each mouse was boosted with the same doses of adjuvant and tumor cells. Spleen cells from mice with a serum titer >4,000 were used for fusion. A hybridoma library was established by fusion of spleen cells from the immunized BALB/c mice and myeloma cells (P3/x63·Ag8) at a 5:1 ratio with polyethylene glycol (PEG)-1500 (Sigma-Aldrich) following standard procedures.[28,29] H6-11 mAb was purified from the supernatant of the H6-11 hybridoma cell line using a NAb Protein A/G Spin Column (Thermo Scientific, Rockford, IL) according to the manufacturer's instructions. The concentration of the purified antibody was quantified by measuring the absorbance at 280 nm on a UV−vis Nanodrop spectrophotometer (Nanodrop Technologies Inc., Wilmington, DE).

Immunofluorescence Staining of PC-3 Cells. An immunofluorescence staining assay was used as previously reported to examine the expression of the mAb H6-11 binding antigen in PC-3 prostate cancer cells with or without fixation.[9,18,30] To stain the PC-3 cells, 50 μL of mAb H6-11 at a concentration of 5 μg/mL in PBS was added to the Lab-Tek chamber slide and incubated for 40 min at 37 °C. The slide was washed 3× with PBS, then 50 μL of 1,000× diluted FITC-conjugated goat antimouse IgG in PBS (Jackson Immuno Research Laboratory Inc., West Grove, PA) was added to each well. The slides were incubated for another 40 min at room temperature. Slides were washed with PBS and observed under a confocal fluorescence microscope FV1000 (Olympus America, Center Valley, PA). Slides containing 20 μm sections of PC-3 solid tumors and surrounding normal muscle from xenografts implants were also used for immunofluorescence staining using procedures similar to those for PC-3 cell staining using H6-11 as the primary antibody as described above.

Immunohistochemical Staining of a Tissue Array of Prostate Cancer and Normal Tissue. To confirm the potential clinical utility of mAb H6-11 in prostate cancer, its specificity was evaluated using an array of human prostate cancer and normal tissue. Slide-mounted histologic samples of 40 human prostate carcinoma specimens, 8 samples of normal prostate tissue, and 1 hepatic carcinoma (US Biomax Inc. Rockville, MD) were deparaffinized in xylene and rehydrated through gradient alcohols as described previously.[9,18,30] The slides were further incubated with mAb H6-11 as the primary antibody at a concentration of 5 μg/mL overnight at 4 °C. Avidin−Biotin Complex Detection System (Vector Laboratory) was then used for chromogenic slide development following standard procedures.[9,18,30] The results were classified into the following categories based on staining intensity and percentage: grade 0 or no staining (−); grade 1 or modest staining (+); grade 2 or positive staining (++); grade 3 or strong positive staining (+++).

^{125}I-Labeling of H6-11. Iodogen solid-phase iodination reagent (Thermo Fisher Pierce Scientific Inc., Rockford, IL) was then used for ^{125}I-labeling of H6-11 following the manufacturer's instructions. Briefly, 0.1−0.2 mg of the purified mAb H6-11 in 0.1 mL of 100 mM, pH 7.4, PBS was treated with 1.0 mCi of [^{125}I]NaI (MP Biomedicals, LLC, Santana, CA) in a reaction vessel which had been plated with the Iodogen reagent. Unlabeled small molecules were removed from the radiolabeled product by passing the reaction mixture through a desalting column (Thermo Fisher Pierce Scientific Inc., Rockford, IL). Labeling efficiency was calculated by measuring the radioactivity of bound IgG as a percentage of total radioactivity. The radiochemical yield was 30−40%. To further confirm IgG labeling, radiolabeled antibody samples were loaded onto SDS−PAGE, and the gel was directly developed on the FLA7000 imaging system (GE Healthcare Biosciences, Piscataway, NJ). The light chain and heavy chain of IgG were both visualized using this autoradiography system.

***In Vitro* Autoradiography.** The immunoreactivity of mAb H6-11 to PC-3 prostate cancer xenografts was evaluated through *in vitro* autoradiography studies using the radioiodinated antibody. Slides containing 20 μm sections from snap-frozen PC-3 tumors were incubated with ^{125}I-labeled H6-11 (1 μCi/mL) in PBS at room temperature for 2 h. After washing three times with PBS/0.01% Tween-20, the slides were air-dried. Dry slides were loaded into the Fuji film phosphor imager film cassette for 12 h at 4 °C in the dark before exposing to a phosphorimager screen and capturing with a Fujifilm FLA-7000 imaging system (GE Healthcare). Photostimulated luminescence (PSL) was quantitated with Fuji Image Gauge software.

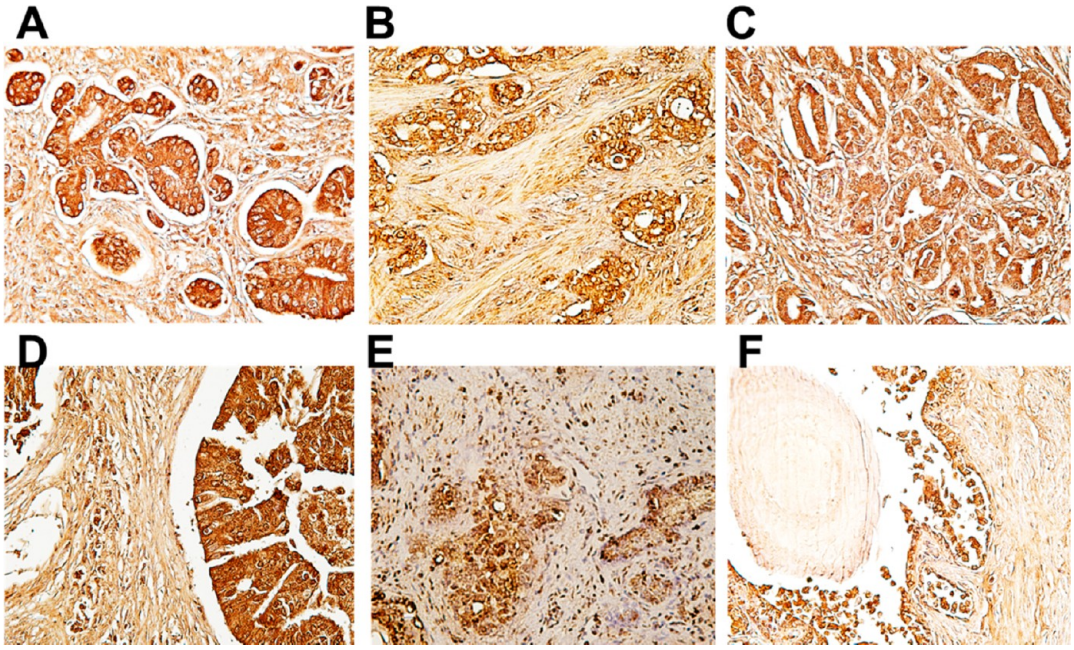

Figure 1. Immunohistochemical staining of mAb H6-11 in different histological grades of prostate cancer (A–E) and in normal prostate tissues (F). (A–E) Different stages of prostate cancer tissues showed positive staining with H6-11. (F) Normal prostate stroma showed negative staining with mAb H6-11, while the prostate gland showed weak positives staining (+).

Characterization of ^{125}I-Labeled H6-11 through Binding Assays. Immunoreactivity of mAb H6-11 was determined by incubating the radioiodinated antibody (≈100,000 cpm) with PC-3 cells (seeded in a 96-well plate at 1×10^5cells/well in PBS/1% FBS). Serial dilutions of ^{125}I-labeled H6-11 (1–133 nM) were added and allowed to incubate for 1 h before the samples were washed with PBS/1% FBS. Three hundred microliters of scintillation cocktail (RPI Corp, Prospect, IL) was added to each well, and the radioactivity of bound antibody was measured with a 1450 MicroBeta Trilux liquid scintillation counter (PerkinElmer Life Health Sciences., Shelton CT). The plot of the bound radioactivity versus the concentration of antibody was fitted to the saturation binding curve using Prism (GraphPad Software Inc., La Jolla, CA), which was used to calculate the binding dissociation constant (K_d) and B_{max}.

Antigen Epitope Characterization by Immunostaining. To characterize the epitope of mAb H6-11, deglycosylation experiments were conducted as previously described[10,17] with some modifications. Briefly, PC-3 or MCF-7 cells were seeded (1×10^5/well) in a 96-well plate, incubated at 37 °C for 48 h, and fixed with 10% neutral buffered formalin for 30 min. After washing twice with PBS and adding 100 μL of a range of concentrations (in triplicate) of sodium periodate (1, 5, 10, and 20 mmol/L in pH 4.5 sodium acetate buffer), trypsin (0.5–2.0 mg/mL in PBS), or deglycosylation reagents (Prozyme Inc., Hayward, CA) into each well of the 96-well plate, the plates were incubated at 37 °C for 2 h for sodium periodate, 1 h for trypsin, and 24 h for the plate treated with deglycosylation reagents. After washing the fixed cells with PBS containing 10% FBS, mAb H6-11 was added to each well at a concentration of 10 μg/mL; this was followed by incubation for 1 h at 37 °C. The secondary antibody, FITC-conjugated goat antimouse, was incubated with the cells in the plates for 45 min. The 96-well plates were read with a Synergy HT Multi-Detection microplate reader (BioTek US, Winooski, VT).

NIR Labeling and *in Vivo* Optical Imaging of the PC-3 Xenograft. In order to evaluate the potential application of H6-11 as a molecular imaging probe, *in vivo* optical imaging experiments were performed using the mAb H6-11 conjugated with IRDye 800CW. The conjugation of protein and NIR dye was done by using the IRDye 800 Protein Labeling Kit (LI-COR Biosciences, Lincoln, Nebraska) as described previously.[9] Mature male athymic nu/nu mice were subcutaneously implanted with PC-3 tumor cells as previously described.[31,32] Tumor-bearing mice were anesthetized with 2% isoflurane/oxygen and placed on the scanner bed for noninvasive optical imaging of the ventral surface. Then, 100 μg of IRDye 800CW-labeled mAb H6-11 in 100 μL of PBS solution was administered by intravenous (i.v.) tail vein injection, and static images were acquired using the Xenogen IVIS-200 optical imager at the indicated time points (0, 24, 48, 72, 96, and 120 h). Imaging data were collected and analyzed by using Living Imaging 3.6 software (Caliper Life Sciences, Alameda, CA) according to the manufacturer's instructions.

^{89}Zr Production and Antibody Labeling. Because of promising results in the optical imaging study, mAb H6-11 was radiolabeled with ^{89}Zr for microPET imaging. ^{89}Zr was produced via the ^{89}Y(p,n)^{89}Zr nuclear reaction using a CS-15 cyclotron (Cyclotron Corporation, Berkeley, CA) and separated via ion exchange at the Washington University Cyclotron Facility with a specific activity of 8.1 to15.4 GBq/mol. The labeling and purification procedure followed previously published methods.[33,34] Briefly, 50 μL of purified mAb H6-11 (5 mg/mL) was incubated with the bifunctional chelator, *p*-isothiocyanatobenzyl-desferrioxamine (*p*-SCN-Bz-DFO) (Macrocyclics Inc., Dallas, TX), in 0.1 M $NaHCO_3$ buffer (pH 9.0) at 4 °C overnight. The product, *p*-SCN-Bz-DFO-H6-11, was purified via Zeba Spin desalting columns (Pierce Biotechnology, Rockford, IL). ^{89}Zr (in 1.0 M oxalic acid) was then complexed with the *p*-SCN-Bz-DFO-H6-11 at a ratio of 222 MBq/mg (6 mCi/mg) of antibody in 0.5 M HEPES buffer at

dx.doi.org/10.1021/mp400130w | *Mol. Pharmaceutics* XXXX, XXX, XXX–XXX

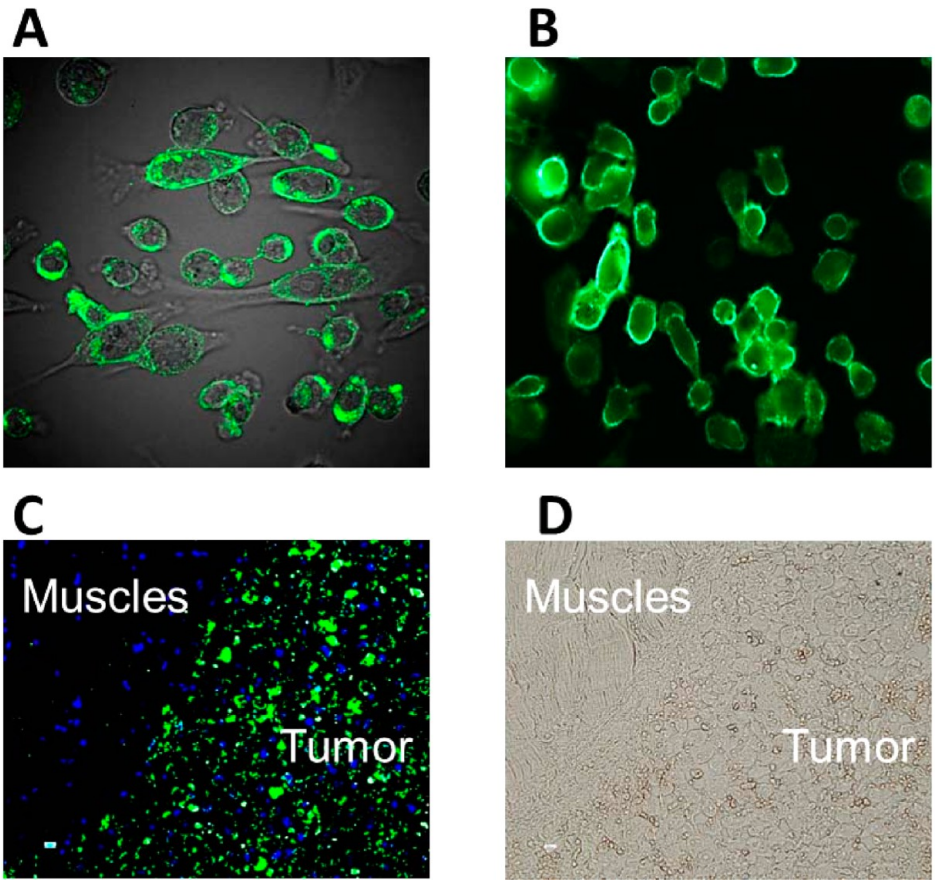

Figure 2. mAb H6-11 immunofluorescence staining of the PC-3 prostate tumor cell line and of PC-3 solid tumor xenografts harvested from nude mice. (A) Human prostate cancer PC-3 cells were fixed with 10% neutral buffered formalin and then immunostained with H6-11. (B) Unfixed PC-3 cells were directly immunostained with H6-11. (C) Immunostaining of PC-3 solid tumors with H6-11. The blue color is the DPI staining for nucleic acid. (D) Bright field of panel C.

pH 7.0 at 37 °C for 1 h with constant agitation. ^{89}Zr-*p*-SCN-Bz-DFO-H6-11 was purified with a Zeba Spin desalting column, and the radiochemical purity was determined by radio-TLC (silica) using a mobile phase of 50 mM diethylenetriamine pentaacetic acid (DTPA) and confirmed with SDS–PAGE autoradiography. The specific activity was ~1 μCi/μg.

MicroPET Imaging. PC-3 tumors were implanted subcutaneously in male athymic nu/nu mice as previously described.[31,32] For microPET imaging using an Inveon MicroPET/CT scanner (Siemens Inc., Knoxville, TN), mice were anesthetized with 2% isoflurane/oxygen, positioned side-by-side in a custom bed, and tail vein catheters were placed. Tumor-bearing mice (n = 2) were injected with 150 μCi/100 μL ^{89}Zr-labeled H6-11 in saline. Initial 30 min dynamic images was acquired; subsequent 30 min static images were obtained at 4, 24, 48, 72, 96, and 120 h postinjection. PET images were coregistered with CT using image display software (Inveon Research Workplace, Siemens). Acquisition time for CT data was 10 min (1 bed position), and images were reconstructed using a filtered back projection reconstruction algorithm and displayed using the ASIPro VM software package, version 4.0 (Siemens Medical Solutions USA, Inc.).

RESULTS

Immunohistochemical Staining of a Tissue Array of Prostate Cancer and Normal Tissue. We previously screened other antibodies from our hybridoma library; several of those antibodies showed tumor specificity and potential for *in vivo* molecular imaging applications.[9,18,30] In this study, we first identified the novel mAb H6-11 by screening hybridoma libraries against human colon adenocarcinoma NSY42129 cells. We have previously reported that antibodies produced from mice immunized with this cell line also recognize surface antigens associated with other tumor types.[9,18,35] An array of 40 clinical human prostate cancer samples and 8 healthy human prostate tissues was used to determine the potential utility of the novel mAb H6-11 for the detection of prostate cancer. At first, we examined the reactivity of the antibody to human prostate cancer tissues to determine the sensitivity and accuracy of the epitope targeted by mAb H6-11. We found that 95% (38 of 40 adenocarcinoma cases) showed positive staining with H6-11. +, ++, and +++ were 20%, 45%, and 30%, respectively (Supporting Information, Tables S1 and S2). All of the prostate adenocarcinoma cases tested exhibited intense homogeneous staining; furthermore, the epitope recognized by H6-11 was expressed in all histologic grades of prostate cancers, as shown in Figure 1. In order to demonstrate specificity to tumor tissue, we also tested H6-11 with eight samples of normal prostate tissue. Our results showed that the mAb H6-11 binding was undetectable in fibromuscular stroma from healthy prostate glands, although weak positive staining was observed in the prostate epithelium (Figure 1 and Supporting Information, Table S1).

***In Vitro* Autoradiography with ^{125}I-H6-11.** Radiolabeling of the novel mAb H6-11 with iodine-125 permitted further

dx.doi.org/10.1021/mp400130w | *Mol. Pharmaceutics* XXXX, XXX, XXX–XXX

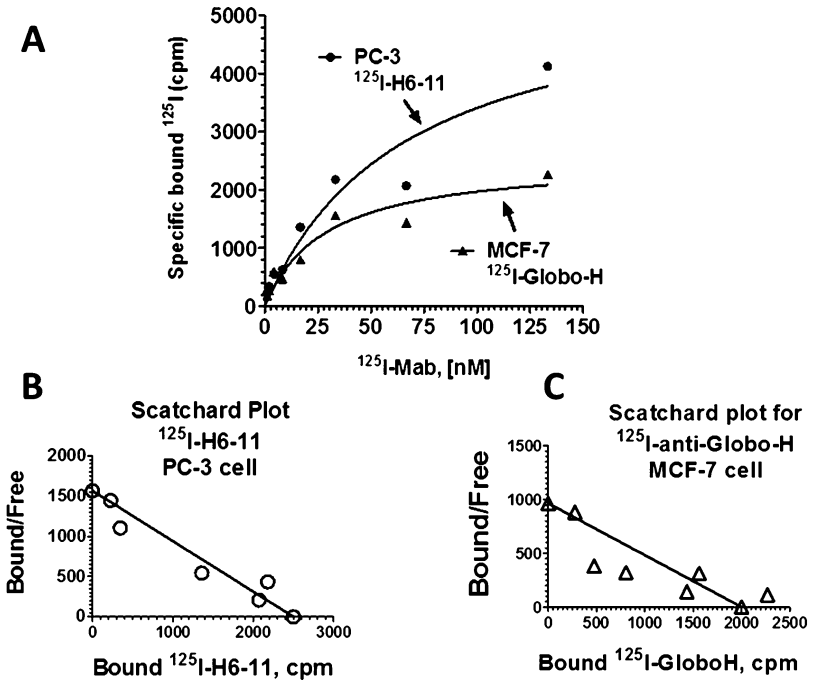

Figure 3. Radioactive ligand saturation binding studies with ^{125}I-labeled H6-11. (A) Variable concentrations of ^{125}I–labeled H6-11 incubated with a constant number of PC-3 prostate cancer cells (●). As a positive control, variable concentrations of ^{125}I-anti-Globo-H antibody were incubated with a constant number of MCF-7 breast cancer cells (▲). (B) The B_{max} and K_d values were estimated from the Scatchard plot for the binding of ^{125}I–H6-11 to PC-3 cells, and (C) Scatchard plot for the binding of ^{125}I-anti-Globo-H antibody to breast cancer MCF-7 cells.

investigations. SDS–PAGE autoradiography of ^{125}I-labeled mAb H6-11 indicated the IgG molecule was iodinated on both the heavy chain and light chain (Supporting Information, Figure S1). Additional *in vitro* autoradiography studies were carried out with slides containing sectioned PC-3 tumor tissue and surrounding normal muscle from snap-frozen xenograft implants. ^{125}I-Labeled intact purified mouse IgG (mIgG) was used as the negative control, and glycolipid-specific antibody anti-Globo-H (MBr1)[14–16] (Enzo Life Sciences, Inc., Farmingdale, NY) was used as a positive control. ^{125}I-mIgG showed no detectable interaction with either the tumor or the muscle. ^{125}I-Globo-H reacted with both the tumor and muscle equally, while ^{125}I–H6-11 reacted strongly to PC-3 solid tumors but showed no binding to muscle. (Supporting Information, Figure S2) These results are consistent with the observation that in immunofluorescence staining, H6-11 preferentially bound to PC-3 prostate cancer cells from culture and solid tumors but showed little binding in the surrounding muscle and stroma (Figure 2).

Immunofluorescence Staining of PC-3 Cells. We performed immunofluorescence staining on cultured PC-3 cells with and without fixation to determine if mAb H6-11 antigen is expressed on the cell surface. Typical ring-like intense cell membrane staining was observed in cultured live PC-3 cells without fixation (Figure 2A). When PC-3 cells were fixed with 10% neutral buffered formalin, both the surface and cytoplasmic regions were intensively positive (Figure 2B). This suggests that the antigen to which mAb H6-11 binds may not only be located on the surface of the tumor cells but that it may also be present in the cytoplasm. As noted above, PC-3 solid tumor xenografts and normal muscle tissue which were snap-frozen and mounted on glass slides for incubation with mAb H6-11 and subsequent immunofluorescence staining also showed preferential and strong binding of the mAb to the tumor cells with little binding to the normal tissue (Figure 2C and D).

Characterization of ^{125}I-Labeled H6-11 through Binding Assays. To qualitatively study the binding of the novel mAb H6-11 to human prostate cancer, ^{125}I-labeled H6-11 was used to measure the K_d and B_{max} with PC-3 cells. Variable concentrations of ^{125}I-labeled H6-11 were incubated with 1×10^5 PC-3 cells, then the unbound mAb was washed away, and the radioactivity which remained and was specifically bound to prostate cancer cells was measured on a liquid scintillation counter. On the basis of radioactivity saturation binding curve fitting (Figure 3), the estimated B_{max} is 5651 ± 1320 cpm/1×10^5 cell, and specific binding K_d is 61.7 ± 30 nM. As a positive control, ^{125}I-labeled anti-Globo-H was similarly incubated with MCF-7 breast cancer cells, and specific binding was determined by the same procedure (Figure 3). Globo-H binding to MCF-7 cells showed B_{max} = 2536 ± 374 cpm/1×10^5 cell, and K_d = 26.9 ± 11 nM. The K_d for H6-11 and PC-3 is close to the K_d for Globo-H and MCF-7, indicating that mAb H6-11 has typical antigen–antibody binding to the PC-3 cells.

Antigen Epitope Characterization by Immunostaining. In general, most cell surface antigens with which antibodies react are glycoproteins or glycolipids, i.e., CA-199, CA-125, and Globo-H.[8,15,36,37] To further explore if the antigen of H6-11 is a glycoprotein or glycolipid, the epitope was characterized by deglycosylation experiments. We treated PC-3 and MCF-7 cells with different concentrations of trypsin, followed by radioactivity measurement using ^{125}I-labeled H6-11 and anti-Globo-H (MBr1), respectively. Because anti-Globo-H antibody recognizes the glycolipid antigens on the surface of MCF-7, the immunoreactivity was not affected by trypsin digestion (Supporting Information, Figure S3C). However, bound radioactivity significantly decreased with trypsin treatment of PC-3 cells (Supporting Information, Figure S3A).

dx.doi.org/10.1021/mp400130w | *Mol. Pharmaceutics* XXXX, XXX, XXX–XXX

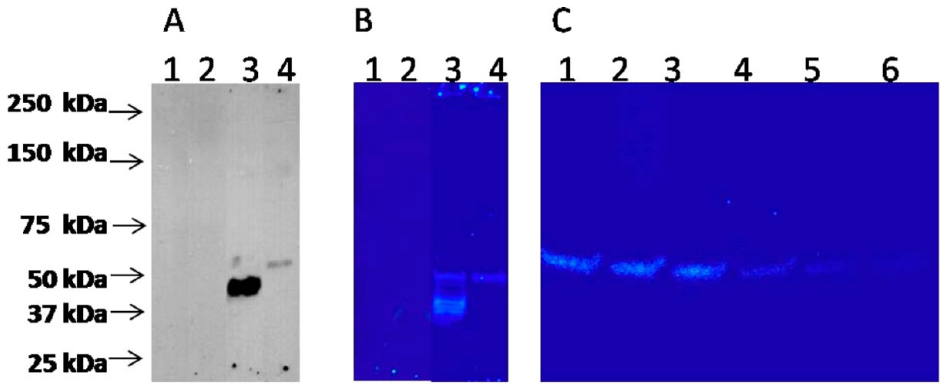

Figure 4. *O*-GlcNAc is the main glycosylation structure of the H6-11 antigenic epitope. (A) Breast cancer cell line MCF-7 (lanes 1 and 3) and prostate cancer cell line PC-3 (lanes 2 and 4) were lysed and subjected to western blot analysis with anti-Globo-H antibody (lanes 1 and 2) and H6-11 (lanes 3 and 4) as the primary antibody and HRP-labeled anti mouse IgG as the secondary antibody. (B) Breast cancer cell line MCF-7 (lanes 1 and 3) and prostate cancer cell line PC-3 (lanes 2 and 4) were lysed and subjected to western blot analysis with ^{125}I-labeled anti-Globo-H antibody (lanes 1 and 2) and H6-11 (lanes 3 and 4), respectively. (C) PC-3 cell line lysate was digested with 5 different deglycosylation enzymes (lane 1, uncut control; lane 2, *N*-glycanase PNGase F; lane 3, sialidase A; lane 4, *O*-glycanase; lane 5, β(1−4) galactosidase; and lane 6, β-*N*-acetyl glucosaminidase) and subjected to western blot analysis using ^{125}I-labeled H6-11.

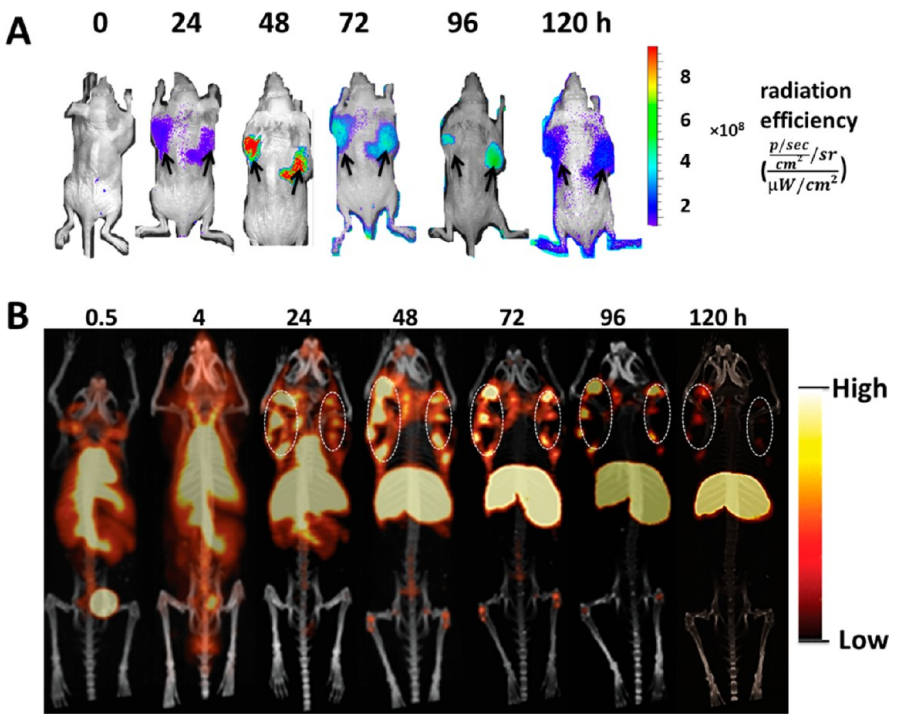

Figure 5. *In vivo* molecular imaging of PC-3 tumor-bearing athymic mice. (A) H6-11-IRDye 800CW optical imaging of PC-3 tumor-bearing mice at 0, 24, 48, 72, 96, and 120 h postinjection. The maximum tumor uptake is around 48−72 h. The black arrows indicate the tumors. (B) ^{89}Zr-labeled H6-11 microPET coronal imaging of PC-3 tumor-bearing mice at 0.5, 4, 24, 48, 72, 96, and 120 h postinjection. The dashed white circles are the bilaterally implanted tumors. A scale bar is shown beside each image.

When the antigen on PC-3 was digested with trypsin, the polypeptide portion of the antigen was truncated; thus, the bound radioactivity decreased. This suggested that the H6-11 antigen contains a polypeptide that can be digested by trypsin. We also treated tumor cells with different concentrations of sodium periodate, followed by radioactivity measurement using ^{125}I-labeled H6-11 for PC-3 and ^{125}I-anti-Globo-H for MCF-7. Both experiments produced an increasing bound radioactivity suggesting that both antigens contain a glycan portion (Supporting Information, Figure S3B and D). Similar experiments have been reported previously;[10] periodate treatment uncovers the carbohydrate groups on the glycan, thus facilitating the antibody's access to the buried antigenic epitopes.

Glycoprotein Antigen Identification. To further identify the glycoprotein antigen, we lysed MCF-7 and PC-3 cell pellets, collected the membrane and cytoplasmic proteins, and then conducted western blot analysis using mAb H6-11 as a primary antibody. No distinct band was identified in the membrane-extracted proteins (data not shown), but proteins with an extremely high molecular weight lack mobility in SDS−PAGE. In contrast, soluble protein bands from cytoplasmic extractions of both MCF-7 and PC-3 cell pellets were identified (Figure 4A). Multiple bands from 40 to 50 kDa were observed from

dx.doi.org/10.1021/mp400130w | *Mol. Pharmaceutics* XXXX, XXX, XXX−XXX

MCF-7 cytoplasmic proteins, while PC-3 showed a single cytoplasmic protein band. ^{125}I-labeled mAb H6-11 autoradiography (Figure 4B) confirmed that a single protein band was responsible for the immunoreactivity of mAb H6-11 to PC-3 versus the multiple protein bands, which were seen in MCF-7.

β-*N*-Acetylglucoside Glycosylation of H6-11 Antigen. To further explore the glycan type of H6-11 antigen epitope, we performed deglycosylation experiments. PC-3 cell lysates were digested with five different deglycosylation enzymes: *N*-glycanase PNGase F, sialidase A, *O*-glycanase, β(1−4) galactosidase, and β-*N*-acetylglucosaminidase and then subjected to western blot analysis using ^{125}I-labeled mAb H6-11; gels were analyzed by autoradiography. The untreated lysate showed a clear band around 50 kDa; deglycosylation enzyme treatments using either *N*-glycanase PNGase F or sialidase A generated no significant changes (Figure 4C). When the cell lysate was treated with O-glycanase or β(1−4) galactosidase, the intensity of the 50 kDa band was slightly decreased, suggesting that the antigen epitope glycan is O-linked, rather than N-linked. When the PC-3 cell lysate was treated with β-*N*-acetylglucosaminidase (*O*-GlcNAc), the 50 kDa band disappeared (Figure 4C) suggesting that the *O*-GlcNAc is the main glycosylation structure of the H6-11 antigenic epitope.

***In Vivo* Optical Imaging of H6-11 Labeled with NIR Dye.** A number of *O*-GlcNAc modified targets have been associated with various cancer types.[38−41] Recent studies suggested that *O*-GlcNAc transferase is overexpressed in prostate cancer compared with that in normal prostate epithelium.[39,42] The novel mAb H6-11 specifically recognized *O*-GlcNAc antigens; thus, we hypothesized that H6-11 would be a good imaging agent for prostate cancer. Therefore, we labeled mAb H6-11 with IRDye 800CW and conducted NIR imaging studies to determine the biodistribution and kinetic changes of the H6-11-IRDye 800CW conjugate in PC-3 tumor-bearing nude mice. As demonstrated in Figure 5A, the bilateral tumors were clearly visible 24 h postinjection. The fluorescence intensity of the tumor region was highest 48 h postinjection. The rapid clearance from nontarget regions and accumulation of this imaging probe in the xenograft prostate tumors resulted in high quality images, with good contrast even 120 h postinjection (Figure 5A).

MicroPET Studies. Because of the promising results of optical imaging, we decided to continue our exploration of *in vivo* imaging using microPET. Optical imaging is limited to shallow surface tissues due to the low penetration of fluorescent signals; thus, PET is a preferred modality for clinical studies. The novel mAb H6-11 was successfully conjugated with the chelator *p*-SCN-Bz-DFO and labeled with ^{89}Zr in 97% radiochemical yield. Both heavy and light chains showed ^{89}Zr labeling (Supporting Information, Figure S4). Chelation with *p*-SCN-Bz-DFO did not alter the immunoreactivity of H6-11 (Supporting Information, Figure S5). At different time points postinjection of ^{89}Zr−H6-11, static microPET scans were performed. Quantitative analysis of the images showed that the uptake gradually increased in the tumor tissue and decreased in the liver and heart until 48−72 h (Figure 5B). The tumor signal persisted at least 120 h postinjection (Figure 5B). This result was consistent with the optical imaging studies. In addition, microPET imaging showed that uptake was limited to the outer regions of the tumor; the tracer did not penetrate to the center of the solid tumor which suggests that *in vivo* tracer uptake may reflect differences in the tumor microenvironment (Figure 5B). The center area of the tumor was confirmed by histology as necrotic tumor tissue.[43,44] Similar phenomena have been reported previously.[43−46]

DISCUSSION

One of the most common changes in glycosylation for cancer cells is an increase in the side branching of N-linked or O-linked glycans.[42,47,48] This increased branching creates additional sites for terminal sialic acid residues, which, in combination with an up-regulation of sialyltransferases, leads to an increase in global sialylation, which is commonly associated with cancer development and progression. Glycosyl transferases (e.g., sialyl transferases and fucosyl transferases) involved in adding terminating residues to glycan tend to be overexpressed in breast cancer and prostate cancer.[37] The increased activity of these glycosyl transferases leads to an increase in certain terminal glycans. Glycan residues commonly found on transformed cells include sialyl Lewis^X, sialyl Tn, Globo-H, and polysialic acid. Many of these glycans have been observed in malignant cancer tissues.[2,13,15,37,49]

The addition of *O*-glycosidic GlcNAc in β linkage to Ser/Thr residues (*O*-GlcNAc) is a dynamic post-translational modification that occurs on numerous cytoplasmic and nuclear proteins and is distinct from complex carbohydrate synthesis in the secretory pathway.[42] Previous studies suggested that altered *O*-GlcNAcylation may play an important role in the pathogenesis of diabetes mellitus,[50,51] etiology of Alzheimer's disease,[50−52] and breast cancer development.[38,40,53] Recent studies suggested that *O*-GlcNAc modification is elevated in prostate cancer due to the overexpression of *O*-GlcNAc transferase in prostate cancer compared to that in normal prostate epithelium.[39,42] In this study, we found that the novel mAb H6-11 detected 95% of the prostate adenocarcinomas in a tissue array and specifically bound to the PC-3 human prostate cancer cell line. H6-11 also showed stronger immunostaining in PC-3 tumor xenografts than in the surrounding muscle (Figure 2). Subsequent *in vivo* optical and microPET imaging of PC-3 tumor-bearing nude mice confirmed that H6-11 was retained in the tumor and washed out of the muscle (Figure 5). These results are consistent with previous publications that *O*-GlcNAc glycosylation modification occurs more frequently in tumors than in normal muscle tissue.[42,47,48]

Biochemical analysis of the cytoplasm of different cell lines revealed that the antigen from the cytoplasm of PC-3 cells is a soluble glycoprotein with molecular weight ∼50 kDa (Figure 4). The glycosylation of this antigen was confirmed to be *O*-GlcNAc (Figure 4C). Since both the breast cancer cell MCF-7 and the colon cancer cell line NSY42129 showed a positive reaction to H6-11 (Figure 4 and Supporting Information, Figure S2), and the epithelial cells from healthy prostate tissues also showed positive staining with H6-11 (Supporting Information, Table S1), we determined that the antigen recognized by H6-11 is not specific to prostate cancer. When we radiolabeled H6-11 with NIR dye and ^{89}Zr for *in vivo* imaging, our results in PC-3 tumor-bearing mice suggested that the *O*-GlcNAc-specific antibody (such as H6-11) is a good candidate for a cancer imaging agent because it showed good discrimination between tumor and normal tissues.

Cell surface antigens are easily accessible for binding to ligands including antibodies for tumor-targeted imaging and therapy. The binding of mAb H6-11 to living (cultured) cells indicates that the epitope recognized by the antibody is localized on cell membranes because living cells only allow

surface molecules to be detected in immunofluorescent staining. When the PC-3 cells were stained after fixation, the cytoplasmic antigens also showed a strong green fluorescent signal indicating that the *O*-GlcNAc-modified glycoprotein antigens are present not only on the surface of the tumor cells but also in the cytoplasm (Figure 2). This observation is consistent with the ~50 kDa band, which was clearly visualized by western blot analysis of soluble cytoplasmic proteins (Figure 4). Further mass spectrometry characterization of this unknown protein is underway, and may identify a new *O*-GlcNAc-modified antigen which binds to prostate and other cancers.

A major motivation for identifying tumor-specific ligands is to improve the diagnosis and treatment of cancer. Preclinical evaluation of imaging and therapeutic agents in animal models is a critical step for developing biological reagents for future clinical use. In tumor (n = 40) and normal tissue (n = 8) array analysis, the novel mAb H6-11 bound to ~95% of 40 different human prostate cancer tissue samples representing different disease stages or grades (Supporting Information, Figure S1). Although strong positive staining was observed, there was no positive correlation between disease stage and the staining intensity (Supporting Information, Figure S1). Normal prostate fibromuscular stroma showed negative mAb H6-11 staining (Figure 1). These results imply that mAb H6-11 is a good candidate for developing a biological imaging agent for the detection of prostate cancer or monitoring response to therapy. In this study, we observed that the probes accumulate in the tumor within 24 h postinjection and were retained in the tumor for at least 120 h.

We found that once an imaging probe is taken up in the xenograft prostate tumor, it accumulates and is retained during the period of washout from normal organs and tissues including the liver and kidney (Figure 5). H6-11-based imaging and therapeutic agents may be capable of detecting subclinical tumors *in vivo* and efficiently delivering anticancer drugs to the tumor cells. Conjugates of antibodies with imaging agents generally have high binding affinity and specificity. They are also retained in the tumor for a much longer time than smaller peptide-based imaging and therapeutic agents. An inherent disadvantage is that more time is required for clearance from normal tissues and organs. There are also concerns about the diffusion of antibody-based imaging and therapeutic reagents into deep tumor tissues where there is a higher interstitial fluid pressure and heterogeneous blood supply. Our microPET studies suggest that hypoxia or necrotic tissues prevent probe accumulation (Figure 5). This may limit the application of H6-11 for tumor imaging. Currently, we have sequenced the cDNA of the hybridoma cell line for H6-11 (Supporting Information, Figure S6); we can optimize the binding properties by antibody engineering as previously reported by other groups to improve tumor image quality.[54−56] Furthermore, mAb H6-11 conjugated with NIR fluorophores could be used to identify small masses associated with subclinical metastatic disease in the peritoneal region before and during surgery. Many prostate cancer patients (including Stage I patients) have unsuspected subclinical metastasis. Identifying subclinical tumors will help the physician to properly manage the disease and improve patient survival.

In summary, we characterized a novel mAb, H6-11, that specifically recognizes a ~50 kDa *O*-GlcNAc-modified glycoprotein found in PC-3 cancer cells. The K_d and B_{max} values measured for the ^{125}I-labled novel mAb with PC-3 tumor cells were similar to the values determined for Globo-H and MCF-7 cells, indicating that H6-11 displays typical antibody−antigen binding. Molecular imaging techniques with two different H6-11 probes demonstrated good tumor to muscle contrast in PC-3 tumor-bearing nude mice using both NIR fluorescence and microPET imaging. This data collectively supports future studies on the application of a TACA-recognizing monoclonal antibody such as H6-11 for prostate tumor detection and imaging.

■ ASSOCIATED CONTENT

Supporting Information

Immunostaining data, immunoreactivity data, autoradiogrrarphic study results, and amino acid sequence for the CDRs region of H-11 hybridoma cell line. This material is available free of charge via the Internet at http://pubs.acs.org.

■ AUTHOR INFORMATION

Corresponding Author

*Department of Radiology, Washington University School of Medicine, Campus Box 8225, 510 S. Kingshighway Blvd., St. Louis, MO 63110, USA. Tel: 1-314-362-8487. Fax: 1-314-362-8555. E-mail: tuz@mir.wustl.edu.

Notes

The authors declare no competing financial interest.

■ ACKNOWLEDGMENTS

We appreciate the radionuclide production by the cyclotron facility at Washington University in St. Louis. We thank Nicole Fettig, Amanda Roth, Lori Strong, and Margaret Morris for their technical help and also Small Animal Imaging Facility of Washington University in St. Louis. We also appreciate Baogang Xu for the helpful discussions regarding the iodination experiment. We thank Lynne Jones for editing assistance. Experimental support was also provided by the Hybridoma Facility of the Rheumatic Diseases Core Center (NIH P03AR048335). Grant support: US Department of Defense, BCRP Award W81XWH-10-1-0031; and NIH grants R01 NS 075527 and R21 MH 092797.

■ ABBREVIATIONS

CT, computed tomography; CDR, complementarity-determining regions; DTPA, diethylenetriamine pentaacetic acid; FCS, fetal calf serum; HE, human epididymis; h, hour; i.v., intravenous injection; i.p., intraperitoneal injection; kDa, kilodalton; mAb, monoclonal antibody; NIR, near-infrared; *O*-GlcNAc, O-linked *β*-*N*-acetylglucosamine; *p*-SCN-Bz-DFO, *p*-isothiocyanatobenzyl-desferrioxamine; PBS, phosphate buffered saline; PEG, polyethylene glycol; PSL, photostimulated luminescence; PET, positron emission tomography; SPECT, single photon emission computed tomography; SDS−PAGE, sodium dodecyl sulfate−polyacrylamide gel electrophoresis; TACA, tumor-associated carbohydrate antigen; TLC, thin layer chromatography

■ REFERENCES

(1) Tesarova, P.; Kalousova, M.; Trnkova, B.; Soukupova, J.; Argalasova, S.; Mestek, O.; Petruzelka, L.; Zima, T. Carbonyl and oxidative stress in patients with breast cancer–is there a relation to the stage of the disease? *Neoplasma* **2007**, *54* (3), 219−224.

(2) Kumar, S. R.; Sauter, E. R.; Quinn, T. P.; Deutscher, S. L. Thomsen-Friedenreich and Tn antigens in nipple fluid: Carbohydrate biomarkers for breast cancer detection. *Clin. Cancer Res.* **2005**, *11* (19 Pt 1), 6868−6871.

(3) Glinskii, O. V.; Sud, S.; Mossine, V. V.; Mawhinney, T. P.; Anthony, D. C.; Glinsky, G. V.; Pienta, K. J.; Glinsky, V. V. Inhibition of prostate cancer bone metastasis by synthetic TF antigen mimic/galectin-3 inhibitor lactulose-L-leucine. *Neoplasia (New York, NY)* **2012**, *14* (1), 65−73.
(4) Khabaz, M. N.; McClure, J.; McClure, S.; Stoddart, R. W. Glycophenotype of prostatic carcinomas. *Folia Histochem. Cytobiol.* **2010**, *48* (4), 637−645.
(5) Mariano, A.; Di Carlo, A.; Santonastaso, C.; Oliva, A.; D'Armiento, M.; Macchia, V. Expression of Lewis carbohydrate antigens and chromogranin A in human prostatic cancer. *Int. J. Oncol.* **2000**, *17* (1), 167−171.
(6) Marczynska, A.; Kulpa, J.; Lenko, J.; Bugajski, A.; Wojcik, E. CA-50 serum level in patients with prostate cancer. *Urol. Res.* **1990**, *18* (3), 189−191.
(7) Abel, P. D.; Cornell, C.; Buamah, P. K.; Williams, G. Assessment of serum CA 19.9 as a tumour marker in patients with carcinoma of the bladder and prostate. *Br. J. Urol.* **1987**, *59* (5), 427−429.
(8) Moore, L. E.; Pfeiffer, R. M.; Zhang, Z.; Lu, K. H.; Fung, E. T.; Bast, R. C., Jr. Proteomic biomarkers in combination with CA 125 for detection of epithelial ovarian cancer using prediagnostic serum samples from the Prostate, Lung, Colorectal, and Ovarian (PLCO) Cancer Screening Trial. *Cancer* **2012**, *118* (1), 91−100.
(9) Xu, M.; Yuan, Y.; Xia, Y.; Achilefu, S. Monoclonal antibody CC188 binds a carbohydrate epitope expressed on the surface of both colorectal cancer stem cells and their differentiated progeny. *Clin. Cancer Res.* **2008**, *14* (22), 7461−7469.
(10) Bergeron, A.; LaRue, H.; Fradet, Y. Biochemical analysis of a bladder-cancer-associated mucin: Structural features and epitope characterization. *Biochem. J.* **1997**, *321* (Pt 3), 889−895.
(11) Li, Q.; Anver, M. R.; Butcher, D. O.; Gildersleeve, J. C. Resolving conflicting data on expression of the Tn antigen and implications for clinical trials with cancer vaccines. *Mol. Cancer Ther.* **2009**, *8* (4), 971−979.
(12) Slovin, S. F.; Ragupathi, G.; Musselli, C.; Fernandez, C.; Diani, M.; Verbel, D.; Danishefsky, S.; Livingston, P.; Scher, H. I. Thomsen-Friedenreich (TF) antigen as a target for prostate cancer vaccine: Clinical trial results with TF cluster (c)-KLH plus QS21 conjugate vaccine in patients with biochemically relapsed prostate cancer. *Cancer Immunol. Immunother.* **2005**, *54* (7), 694−702.
(13) Martensson, S.; Bigler, S. A.; Brown, M.; Lange, P. H.; Brawer, M. K.; Hakomori, S. Sialyl-Lewis^x and related carbohydrate antigens in the prostate. *Hum. Pathol.* **1995**, *26* (7), 735−739.
(14) Wang, C. C.; Huang, Y. L.; Ren, C. T.; Lin, C. W.; Hung, J. T.; Yu, J. C.; Yu, A. L.; Wu, C. Y.; Wong, C. H. Glycan microarray of Globo H and related structures for quantitative analysis of breast cancer. *Proc Natl Acad Sci U S A* **2008**, *105* (33), 11661−6.
(15) Chang, W. W.; Lee, C. H.; Lee, P.; Lin, J.; Hsu, C. W.; Hung, J. T.; Lin, J. J.; Yu, J. C.; Shao, L. E.; Yu, J.; Wong, C. H.; Yu, A. L. Expression of Globo H and SSEA3 in breast cancer stem cells and the involvement of fucosyl transferases 1 and 2 in Globo H synthesis. *Proc. Natl. Acad. Sci. U.S.A.* **2008**, *105* (33), 11667−72.
(16) Gilewski, T.; Ragupathi, G.; Bhuta, S.; Williams, L. J.; Musselli, C.; Zhang, X. F.; Bornmann, W. G.; Spassova, M.; Bencsath, K. P.; Panageas, K. S.; Chin, J.; Hudis, C. A.; Norton, L.; Houghton, A. N.; Livingston, P. O.; Danishefsky, S. J. Immunization of metastatic breast cancer patients with a fully synthetic globo H conjugate: A phase I trial. *Proc. Natl. Acad. Sci. U.S.A.* **2001**, *98* (6), 3270−3275.
(17) LaRue, H.; Parent-Vaugeois, C.; Bergeron, A.; Champetier, S.; Fradet, Y. Influence of spatial configuration on the expression of carcinoembryonic antigen and mucin antigens in human bladder cancer. *Int. J. Cancer* **1997**, *71* (6), 986−992.
(18) Xu, M.; Rettig, M. P.; Sudlow, G.; Wang, B.; Akers, W. J.; Cao, D.; Mutch, D. G.; DiPersio, J. F.; Achilefu, S. Preclinical evaluation of Mab CC188 for ovarian cancer imaging. *Int. J. Cancer* **2012**, *131* (6), 1351−1359.
(19) Urban, N.; Thorpe, J. D.; Bergan, L. A.; Forrest, R. M.; Kampani, A. V.; Scholler, N.; O'Briant, K. C.; Anderson, G. L.; Cramer, D. W.; Berg, C. D.; McIntosh, M. W.; Hartge, P.; Drescher, C. W. Potential role of HE4 in multimodal screening for epithelial ovarian cancer. *J. Natl. Cancer Inst.* **2011**, *103* (21), 1630−1634.
(20) Donadio, A. C.; Lobo, C.; Tosina, M.; de la Rosa, V.; Martin-Rufian, M.; Campos-Sandoval, J. A.; Mates, J. M.; Marquez, J.; Alonso, F. J.; Segura, J. A. Antisense glutaminase inhibition modifies the O-GlcNAc pattern and flux through the hexosamine pathway in breast cancer cells. *J. Cell Biochem.* **2008**, *103* (3), 800−811.
(21) Havaki, S.; Kittas, C.; Marinos, E.; Dafni, U.; Sotiropoulou, C.; Voloudakis-Baltatzis, I.; Goutas, N.; Vassilaros, S. D.; Athanasiou, E.; Arvanitis, D. L. Ultrastructural immunostaining of infiltrating ductal breast carcinomas with the monoclonal antibody H: A comparative study with cytokeratin 8. *Ultrastruct. Pathol.* **2003**, *27* (6), 393−407.
(22) Firpo, M. A.; Gay, D. Z.; Granger, S. R.; Scaife, C. L.; DiSario, J. A.; Boucher, K. M.; Mulvihill, S. J. Improved diagnosis of pancreatic adenocarcinoma using haptoglobin and serum amyloid A in a panel screen. *World J. Surg.* **2009**, *33* (4), 716−722.
(23) Zhang, Z.; Yu, Y.; Xu, F.; Berchuck, A.; van Haaften-Day, C.; Havrilesky, L. J.; de Bruijn, H. W.; van der Zee, A. G.; Woolas, R. P.; Jacobs, I. J.; Skates, S.; Chan, D. W.; Bast, R. C., Jr. Combining multiple serum tumor markers improves detection of stage I epithelial ovarian cancer. *Gynecol. Oncol.* **2007**, *107* (3), 526−531.
(24) Chaturvedi, R.; Heimburg, J.; Yan, J.; Koury, S.; Sajjad, M.; Abdel-Nabi, H. H.; Rittenhouse-Olson, K. Tumor immunolocalization using ^{124}I-iodine-labeled JAA-F11 antibody to Thomsen-Friedenreich alpha-linked antigen. *Appl. Radiat. Isot.* **2008**, *66* (3), 278−287.
(25) Lieberman, G.; Buscombe, J. R.; Hilson, A. J.; Reid, W. M.; Thakrar, D.; Maclean, A. B. Preoperative diagnosis of ovarian carcinoma with a novel monoclonal antibody. *Am. J. Obstet. Gynecol.* **2000**, *183* (3), 534−540.
(26) Tibben, J. G.; Massuger, L. F.; Claessens, R. A.; Schijf, C. P.; Pak, K. Y.; Strijk, S. P.; Kenemans, P.; Corstens, F. H. Tumour detection and localization using ^{99m}Tc-labelled OV-TL 3 Fab' in patients suspected of ovarian cancer. *Nucl. Med. Commun.* **1992**, *13* (12), 885−893.
(27) Xu, M.; Wright, W. D.; Higashikubo, R.; Roti, J. L. Chronic thermotolerance with continued cell proliferation. *Int. J. Hyperthermia* **1996**, *12* (5), 645−660 discussion 661−662..
(28) Thean, E. T.; Toh, B. H. Production and characterization of murine monoclonal antibody to human alpha-lactalbumin. *Immunol. Cell Biol.* **1989**, *67* (Pt 1), 41−48.
(29) Mandeville, R.; Dumas, F.; Amarouch, A.; Sidrac-Ghali, S.; Walker, M. C.; Zelechowska, M.; Ajdukovic, I.; Grouix, B. Affinity purification of a high molecular weight human breast cancer-associated antigen identified by the BCD-B4 monoclonal antibody. *Hybridoma* **1987**, *6* (5), 441−451.
(30) Xu, M.; Wang, F.; Gildersleeve, J. C.; Achilefu, S. MAb L9E10 to blood group H2 antigen binds to colon cancer stem cells and inhibits tumor cell migration and invasion. *Hybridoma* **2010**, *29* (4), 355−359.
(31) Jadvar, H.; Xiankui, L.; Shahinian, A.; Park, R.; Tohme, M.; Pinski, J.; Conti, P. S. Glucose metabolism of human prostate cancer mouse xenografts. *Mol. Imaging* **2005**, *4* (2), 91−97.
(32) Zheng, Q. H.; Gardner, T. A.; Raikwar, S.; Kao, C.; Stone, K. L.; Martinez, T. D.; Mock, B. H.; Fei, X.; Wang, J. Q.; Hutchins, G. D. [^{11}C]Choline as a PET biomarker for assessment of prostate cancer tumor models. *Bioorg. Med. Chem.* **2004**, *12* (11), 2887−2893.
(33) Vosjan, M. J. W. D.; Perk, L. R.; Visser, G. W. M.; Budde, M.; Jurek, P.; Kiefer, G. E.; van Dongen, G. A. M. S. Conjugation and radiolabeling of monoclonal antibodies with zirconium-89 for PET imaging using the bifunctional chelate p-isothiocyanatobenzyl-desferrioxamine. *Nat. Protoc.* **2010**, *5* (4), 739−743.
(34) Perk, L. R.; Vosjan, M. J. W. D.; Visser, G. W. M.; Budde, M.; Jurek, P.; Kiefer, G. E.; van Dongen, G. A. M. S. p-Isothiocyanato-benzyl-desferrioxamine: A new bifunctional chelate for facile radio-labeling of monoclonal antibodies with zirconium-89 for immuno-PET imaging. *Eur. J. Nucl. Med. Mol. Imaging* **2010**, *37* (2), 250−259.
(35) Pu, Y.; Wang, W. B.; Xu, M.; Tang, G. C.; Budansky, Y.; Sharanov, M.; Achilefu, S.; Eastham, J. A.; Alfano, R. R. Near infrared photonic finger imager for prostate cancer screening. *Technol. Cancer Res. Treat.* **2011**, *10* (6), 507−517.

(36) Girgis, M. D.; Kenanova, V.; Olafsen, T.; McCabe, K. E.; Wu, A. M.; Tomlinson, J. S. Anti-CA19-9 diabody as a PET imaging probe for pancreas cancer. *J. Surg. Res.* **2011**, *170* (2), 169−78.
(37) Jin, H.; Zangar, R. C. Protein modifications as potential biomarkers in breast cancer. *Biomarker Insights* **2009**, *4*, 191−200.
(38) Rambaruth, N. D.; Greenwell, P.; Dwek, M. V. The lectin Helix pomatia agglutinin recognizes O-GlcNAc containing glycoproteins in human breast cancer. *Glycobiology* **2012**, *22* (6), 839−848.
(39) Lynch, T. P.; Ferrer, C. M.; Jackson, S. R.; Shahriari, K. S.; Vosseller, K.; Reginato, M. J. Critical role of O-Linked beta-N-acetylglucosamine transferase in prostate cancer invasion, angiogenesis, and metastasis. *J. Biol. Chem.* **2012**, *287* (14), 11070−11081.
(40) Krzeslak, A.; Forma, E.; Bernaciak, M.; Romanowicz, H.; Brys, M. Gene expression of O-GlcNAc cycling enzymes in human breast cancers. *Clin. Exp. Med.* **2012**, *12* (1), 61−65.
(41) Mi, W.; Gu, Y.; Han, C.; Liu, H.; Fan, Q.; Zhang, X.; Cong, Q.; Yu, W. O-GlcNAcylation is a novel regulator of lung and colon cancer malignancy. *Biochim. Biophys. Acta* **2011**, *1812* (4), 514−519.
(42) Sayat, R.; Leber, B.; Grubac, V.; Wiltshire, L.; Persad, S. O-GlcNAc-glycosylation of beta-catenin regulates its nuclear localization and transcriptional activity. *Exp. Cell Res.* **2008**, *314* (15), 2774−2787.
(43) Cho, H.; Ackerstaff, E.; Carlin, S.; Lupu, M. E.; Wang, Y.; Rizwan, A.; O'Donoghue, J.; Ling, C. C.; Humm, J. L.; Zanzonico, P. B.; Koutcher, J. A. Noninvasive multimodality imaging of the tumor microenvironment: registered dynamic magnetic resonance imaging and positron emission tomography studies of a preclinical tumor model of tumor hypoxia. *Neoplasia* **2009**, *11* (3), 247−259 2p following 259..
(44) Uehara, H.; Miyagawa, T.; Tjuvajev, J.; Joshi, R.; Beattie, B.; Oku, T.; Finn, R.; Blasberg, R. Imaging experimental brain tumors with 1-aminocyclopentane carboxylic acid and alpha-aminoisobutyric acid: Comparison to fluorodeoxyglucose and diethylenetriaminepenta-acetic acid in morphologically defined tumor regions. *J. Cereb. Blood Flow Metab.* **1997**, *17* (11), 1239−53.
(45) Wakefield, L. M.; Letterio, J. J.; Chen, T.; Danielpour, D.; Allison, R. S.; Pai, L. H.; Denicoff, A. M.; Noone, M. H.; Cowan, K. H.; O'Shaughnessy, J. A.; et al. Transforming growth factor-beta1 circulates in normal human plasma and is unchanged in advanced metastatic breast cancer. *Clin. Cancer Res.* **1995**, *1* (1), 129−136.
(46) Apostolopoulos, V.; Xing, P. X.; Trapani, J. A.; McKenzie, I. F. Production of anti-breast cancer monoclonal antibodies using a glutathione-S-transferase-MUC1 bacterial fusion protein. *Br. J. Cancer* **1993**, *67* (4), 713−720.
(47) Samih, N.; Hovsepian, S.; Notel, F.; Prorok, M.; Zattara-Cannoni, H.; Mathieu, S.; Lombardo, D.; Fayet, G.; El-Battari, A. The impact of N- and O-glycosylation on the functions of Glut-1 transporter in human thyroid anaplastic cells. *Biochim. Biophys. Acta* **2003**, *1621* (1), 92−101.
(48) Heffernan, M.; Lotan, R.; Amos, B.; Palcic, M.; Takano, R.; Dennis, J. W. Branching beta 1−6N-acetylglucosaminetransferases and polylactosamine expression in mouse F9 teratocarcinoma cells and differentiated counterparts. *J. Biol. Chem.* **1993**, *268* (2), 1242−1251.
(49) MacLean, G. D.; Reddish, M.; Koganty, R. R.; Wong, T.; Gandhi, S.; Smolenski, M.; Samuel, J.; Nabholtz, J. M.; Longenecker, B. M. Immunization of breast cancer patients using a synthetic sialyl-Tn glycoconjugate plus Detox adjuvant. *Cancer Immunol. Immunother.* **1993**, *36* (4), 215−222.
(50) Li, X.; Lu, F.; Wang, J. Z.; Gong, C. X. Concurrent alterations of O-GlcNAcylation and phosphorylation of tau in mouse brains during fasting. *Eur. J. Neurosci.* **2006**, *23* (8), 2078−2086.
(51) Robertson, L. A.; Moya, K. L.; Breen, K. C. The potential role of tau protein O-glycosylation in Alzheimer's disease. *J. Alzheimer's Dis.* **2004**, *6* (5), 489−495.
(52) Yao, P. J.; Coleman, P. D. Reduced O-glycosylated clathrin assembly protein AP180: Implication for synaptic vesicle recycling dysfunction in Alzheimer's disease. *Neurosci. Lett.* **1998**, *252* (1), 33−36.
(53) Caldwell, S. A.; Jackson, S. R.; Shahriari, K. S.; Lynch, T. P.; Sethi, G.; Walker, S.; Vosseller, K.; Reginato, M. J. Nutrient sensor O-GlcNAc transferase regulates breast cancer tumorigenesis through targeting of the oncogenic transcription factor FoxM1. *Oncogene* **2010**, *29* (19), 2831−2842.
(54) Olafsen, T.; Wu, A. M. Antibody vectors for imaging. *Semin. Nucl. Med.* **2010**, *40* (3), 167−181.
(55) Wei, L. H.; Olafsen, T.; Radu, C.; Hildebrandt, I. J.; McCoy, M. R.; Phelps, M. E.; Meares, C.; Wu, A. M.; Czernin, J.; Weber, W. A. Engineered antibody fragments with infinite affinity as reporter genes for PET imaging. *J. Nucl. Med.* **2008**, *49* (11), 1828−1835.
(56) Wu, A. M.; Olafsen, T. Antibodies for molecular imaging of cancer. *Cancer J. (Sudbury, MA)* **2008**, *14* (3), 191−197.

Supplementary Information

Preclinical Evaluation of the Novel Monoclonal Antibody H6-11 for Prostate Cancer Imaging

*Hongjun Jin, Mai Xu, Prashanth K. Padakanti, Yongjian Liu, Suzanne Lapi and Zhude Tu**

Department of Radiology, Washington University School of Medicine, St. Louis, MO 63110

*Corresponding Author: Zhude Tu, Department of Radiology, Washington University School of Medicine, St. Louis, MO, 63110, USA. E-mail: tuz@mir.wustl.edu; Tel.: +1-314-362-8487; Fax: +1-314-262-8555

Table of contents

This material is available free of charge via the Internet at http://pubs.acs.org.

Table S1. Immunostaining of tissue array of prostate tumor with H6-11

No	Sex	Age	Organ	Pathology diagnosis	Grade	Stage	TNM	Type	Staining Scores
1	M	72	Prostate	Adenocarcinoma	1	II	T2N0M0	Malignant	+
2	M	64	Prostate	Adenocarcinoma	1	I	T1N0M0	Malignant	+++
3	M	60	Prostate	Adenocarcinoma	1	IV	T4N1M1c	Malignant	++
4	M	66	Prostate	Adenocarcinoma	1	IV	T3N1M1c	Malignant	++
5	M	65	Prostate	Adenocarcinoma	1	II	T2N0M0	Malignant	++
6	M	75	Prostate	Adenocarcinoma	1	IV	T2N1M1c	Malignant	++
7	M	71	Prostate	Adenocarcinoma	2–3	II	T2N0M0	Malignant	+++
8	M	78	Prostate	Adenocarcinoma	2	IV	T3N2M1	Malignant	+++
9	M	74	Prostate	Adenocarcinoma	2	IV	T4N1M1c	Malignant	+
10	M	69	Prostate	Adenocarcinoma	2	III	T3N0M0	Malignant	++
11	M	75	Prostate	Adenocarcinoma	2	IV	T4N1M1	Malignant	++
12	M	69	Prostate	Adenocarcinoma	2	II	T2N0M0	Malignant	+++
13	M	73	Prostate	Adenocarcinoma	2	IV	T3N1M1c	Malignant	+++
14	M	56	Prostate	Adenocarcinoma	2–3	II	T2N0M0	Malignant	+++
15	M	73	Prostate	Adenocarcinoma	2	II	T2N0M0	Malignant	+++
16	M	70	Prostate	Adenocarcinoma	2	III	T3N0M0	Malignant	++
17	M	20	Prostate	Adenocarcinoma	1–2	III	T3N0M0	Malignant	++
18	M	61	Prostate	Adenocarcinoma	1–2	III	T3N1M	Malignant	++

							0		
19	M	73	Prostate	Adenocarcinoma	2	III	T3N0M0	Malignant	+++
20	M	82	Prostate	Adenocarcinoma	2	II	T2N0M0	Malignant	++
21	M	75	Prostate	Adenocarcinoma	3	IV	T4N1M1	Malignant	+
22	M	78	Prostate	Adenocarcinoma	3	IV	T4N1M1b	Malignant	+-
23	M	60	Prostate	Adenocarcinoma	2	IV	T3N1M1b	Malignant	+
24	M	73	Prostate	Adenocarcinoma	2	IV	T3N1M1b	Malignant	+++
25	M	62	Prostate	Adenocarcinoma	2	IV	T3N1M1b	Malignant	+
26	M	51	Prostate	Adenocarcinoma	2	II	T2N0M0	Malignant	++
27	M	62	Prostate	Adenocarcinoma	3	II	T2N0M0	Malignant	+++
28	M	60	Prostate	Adenocarcinoma	2	IV	T3N1M0	Malignant	+++
29	M	68	Prostate	Adenocarcinoma	2	II	T2N0M0	Malignant	++
30	M	64	Prostate	Adenocarcinoma	3	IV	T3N0M1b	Malignant	+
31	M	66	Prostate	Adenocarcinoma	3	II	T2N0M0	Malignant	++
32	M	87	Prostate	Adenocarcinoma	3	II	T2N0M0	Malignant	+
33	M	81	Prostate	Adenocarcinoma	3	III	T3aN0M0	Malignant	+++
34	M	80	Prostate	Adenocarcinoma	3	IV	T4N1M1c	Malignant	++
35	M	76	Prostate	Adenocarcinoma	3	IV	T3N1M1b	Malignant	+-
36	M	73	Prostate	Adenocarcinoma	3	IV	T4N1M1c	Malignant	+
37	M	63	Prostate	Adenocarcinoma	3	IV	T2N1M1b	Malignant	++
38	M	67	Prostate	Adenocarcinoma	3	II	T2N0M0	Malignant	++
39	M	65	Prostate	Adenocarcinoma	3	IV	T2N1M1	Malignant	++
40	M	64	Prostate	Adenocarcinoma	3	II	T2N0M0	Malignant	++
41	M	35	Prostate	Normal prostate tissue	–	–	–	Normal*	+-

42	M	43	Prostate	Normal prostate tissue	–	–	–	Normal*	+-
43	M	19	Prostate	Normal prostate tissue	–	–	–	Normal*	+-
44	M	46	Prostate	Normal prostate tissue	–	–	–	Normal*	+-
45	M	40	Prostate	Normal prostate tissue	–	–	–	Normal*	+-
46	M	28	Prostate	Normal prostate tissue	–	–	–	Normal*	+-
47	M	33	Prostate	Normal prostate tissue	–	–	–	Normal*	+-
48	M	37	Prostate	Normal prostate tissue	–	–	–	Normal*	+-
–	F	55	liver	Hepatocellular liver cancer (tissue marker)	3		T3N0M0	Malignant	+++

*Epithelia from normal prostate glands are positive staining with mAb H6-11, but not from fibromuscular stroma.

Table S2. Summary of monoclonal antibody H6-11 reactivity with human prostate tumor tissues

Scoring grade	-	±	+	++	+++	Total
Prostate tumor Case (%)	0 (0%)	2 (5%)	8 (20%)	18 (45%)	12 (30%)	40 (100%)
				38 (95%)		

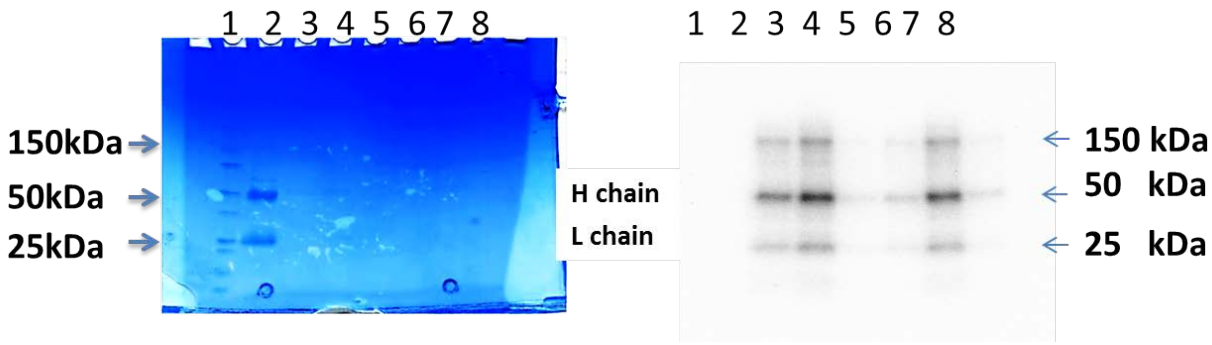

Figure S1. SDS-PAGE (left) and autoradiography (right) of ^{125}I-H6-11.

Lane 1: standard protein marker; Lane 2: unlabeled IgG; Lanes 3-5: ^{125}I labeled H6-11 sample 1 elution 1-3; Lane 6-8: ^{125}I labeled H6-11 sample 2 elution 1-3. Autoradiography from ^{125}I labeled H6-11, two samples, both showed full length IgG (150 KDa), and heavy chain (50 KDa) and light chain (25 KDa) bands indicating successful iodination.

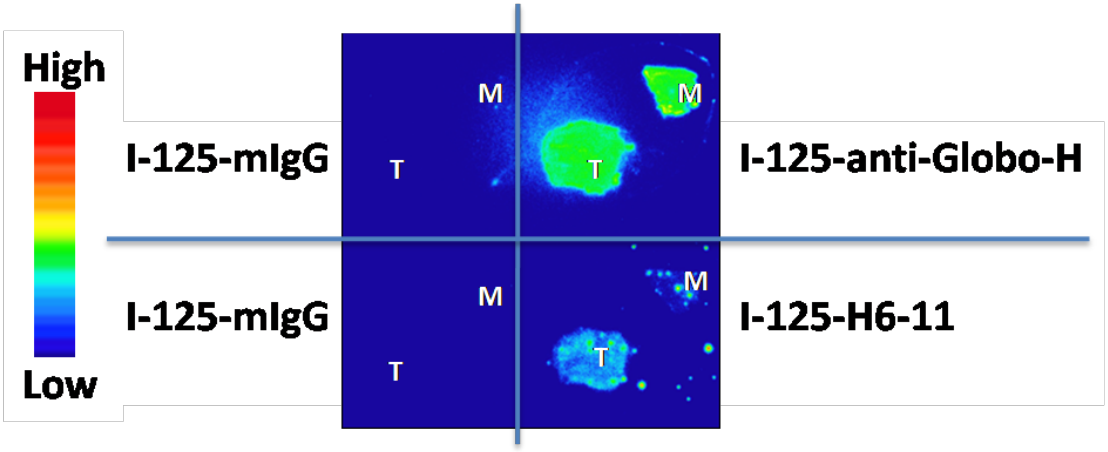

Figure S2. *In vitro* autoradiography of ^{125}I--H6-11 with tumor tissue.

1 μCi/mL ^{125}I labeled mouse IgG, H6-11 and anti-Globo-H antibodies were incubated with tissue slides collected from PC-3 implanted tumor (T) or muscle (M). After incubation and washing the slides three times with PBS-TW-20, the slides were directly placed in the FLA-7000 imager to process for autoradiography. ^{125}I-mIgG has no any detectable interaction with either tumor or muscle tissues. ^{125}I-Globo-H reacted with both the tumor and muscle tissues evenly. ^{125}I-H6-11 reacted strongly to tumor collected from PC-3 xenograft mouse.

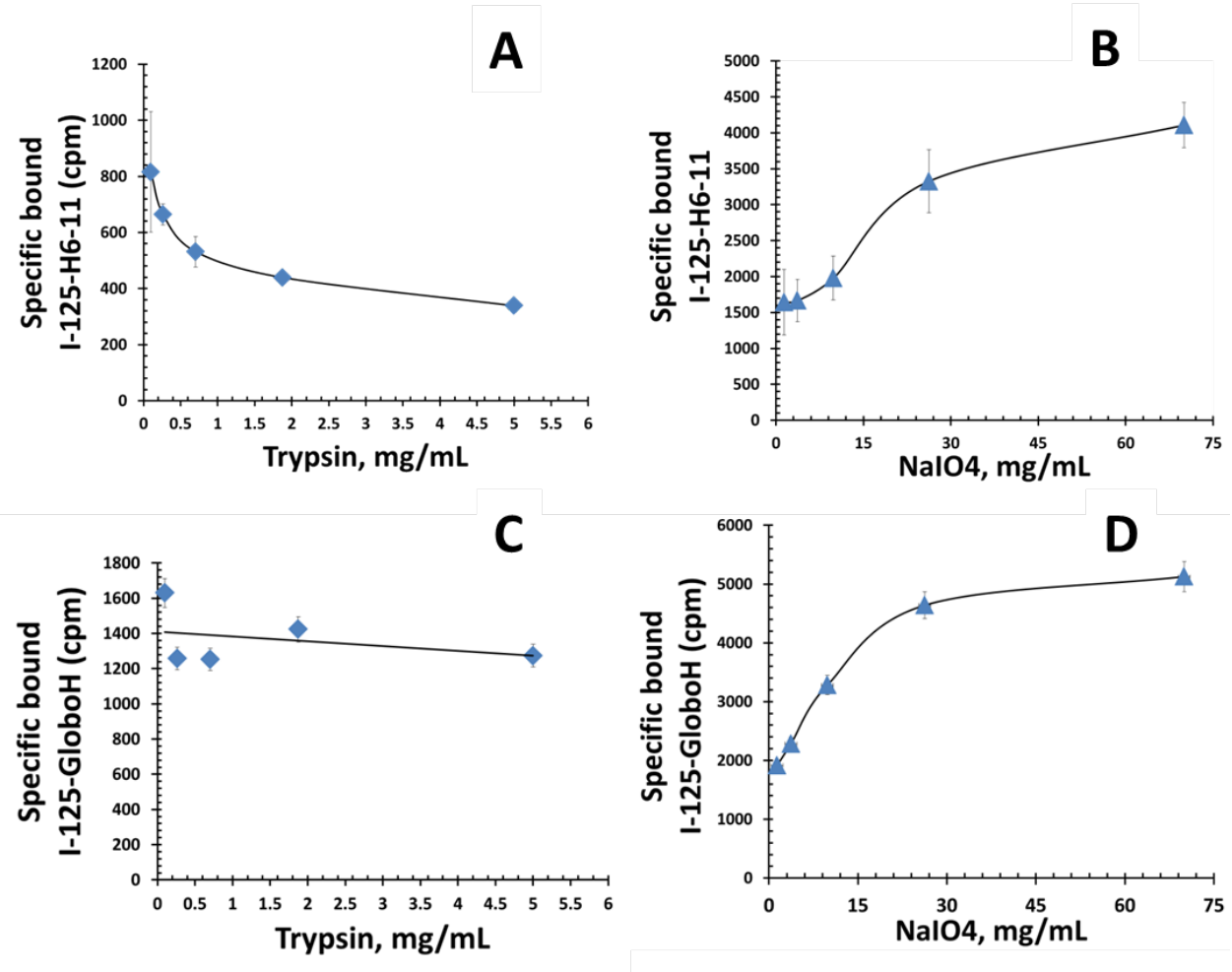

Figure S3. Identification of H6-11antigen epitopes via radioactivity binding measurements with human cancer cells.

Panel A: For PC-3 cells, increasing the concentration of trypsin decreased the ^{125}I-H6-11 binding. **Panel B:** For PC-3 cells, increasing the concentration of periodate increased the ^{125}I-H6-11 binding. **Panel C:** For MCF-7, increasing the concentration of trypsin barely changed the ^{125}I-anti-Globo-H binding. **Panel D**: For MCF-7, increasing the concentration of periodate increased the ^{125}I-anti-Globo-H binding.

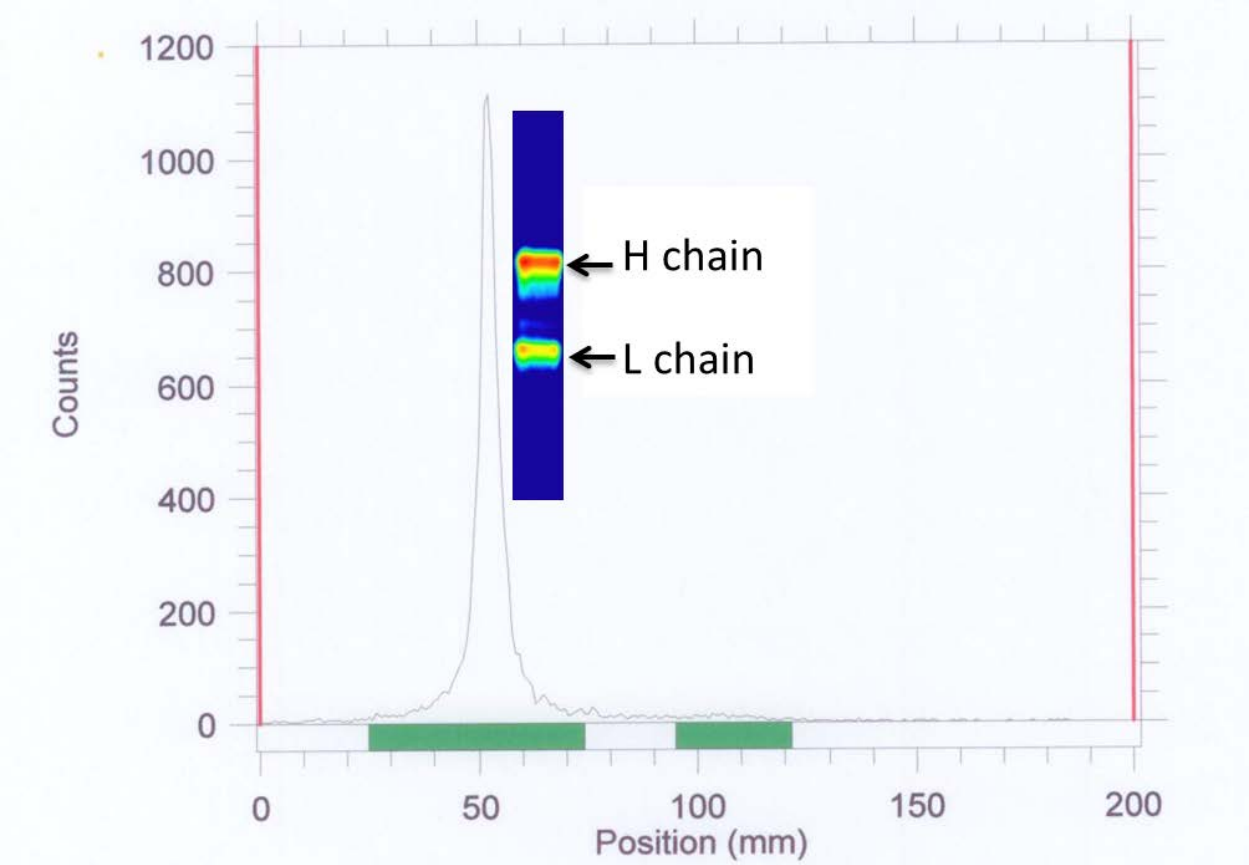

Reg	(mm) Start	(mm) Stop	(mm) Centroid	RF	Region Counts	Region CPM	% of Total	% of ROI
Rgn 1	25.0	74.1	52.4	0.262	8805.0	8805.0	91.15	96.86
Rgn 2	94.8	121.4	106.3	0.531	285.0	285.0	2.95	3.14
2 Peaks					9090.0	9090.0	94.10	100.00

Figure S4. TLC of ^{89}Zr-H6-11 and SDS-PAGE autoradiography.

The ^{89}Zr labeled H6-11 after purification on the Pierce Zeba desalting column was quantified by TLC. The major peak (96.86%) was ^{89}Zr-H6-11 at position 50 mm (baseline), while the free ^{89}Zr peak (3.14%) is at 100 mm position. The inserted image is from the SDS-PAGE and autoradiography of the major peak. Both the heavy and light chains are radiolabeled.

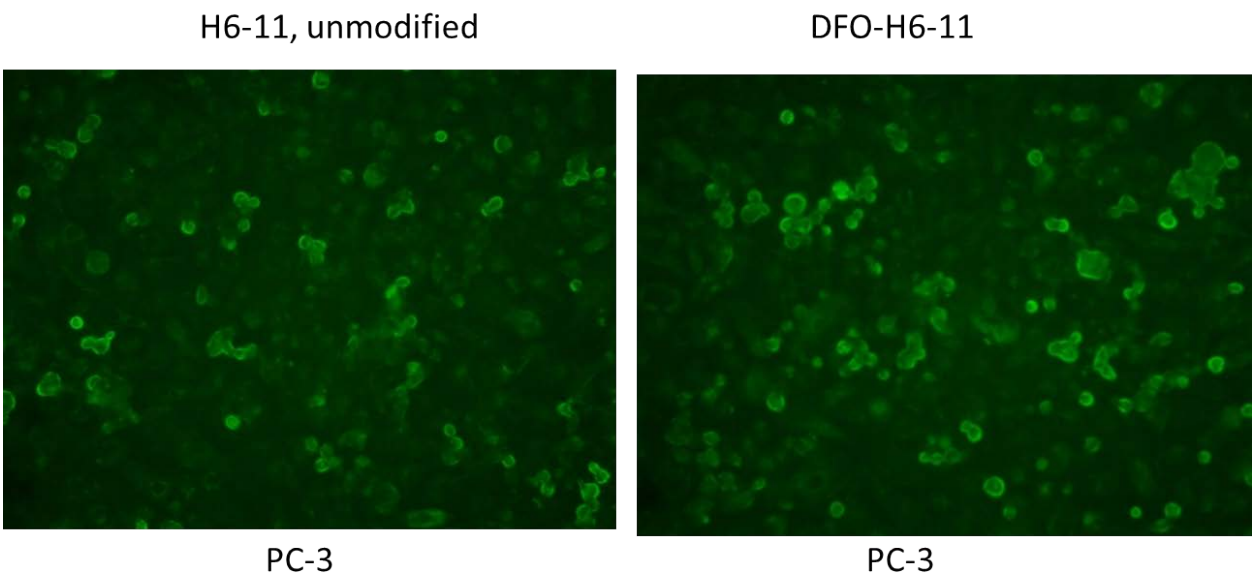

Figure S5. Immunofluorescence of unmodified H6-11 and p-SCN-Bz-DFO modified H6-11.

PC-3 cell was immunofluorescence stained with 5 μg/mL H6-11 (left) and *p*-SCN-Bz-DFO modified H6-11 (abridge: DFO-H6-11) (right). No significant immunoreactivity changes were observed between *p*-SCN-Bz-DFO modified H6-11 and unmodified H6-11.

Heavy chain: Amino acids sequence (135 AA)

Leader sequence-FR1-CDR1-FR2-CDR2-FR3-CDR3-FR4
MAWVWTLLFLMAAAQSIQAQIQLVQSGPELKKPGETVKISCKASGYTF
TDYSMHWVKQAPGKGLKWMGWINTETGEPTYADDFKGRFAFSLETSA
STAYLQINNLKNEDTATYFCARSRRYDDYWGQGTTLTVSS

Light chain: Amino acids sequence (133 AA)

Leader sequence-FR1-CDR1-FR2-CDR2-FR3-CDR3-FR4
MDSQAQVLMLLLLWVSGTCGDIVMSQSPSSLAVSVGEKVTMSCKSSQSL
LYSSNQKNYLAWYQQKPGQSPKLLIYWASTRESGVPDRFTGSGSGTDFTL
TISSVKAEDLAVYYCQQYYSYPYTFGGGTKLEIK

Figure S6. Amino acid sequence for the CDRs region of H6-11 hybridoma cell line.

The amino acid sequences are translated from cDNA sequencings. The predicted binding sites (including heavy chain and light chain) from CDRs were blue coded.

US 20120094860A1

(19) **United States**

(12) **Patent Application Publication**

(10) **Pub. No.: US 2012/0094860 A1**

(43) **Pub. Date: Apr. 19, 2012**

Jin et al.

(54) **COMPOSITIONS, ANTIBODIES, ASTHMA DIAGNOSIS METHODS, AND METHODS FOR PREPARING ANTIBODIES**

(76) Inventors: **Hongjun Jin**, West Richland, WA (US); **Richard C. Zangar**, Richland, WA (US)

(21) Appl. No.: **13/276,608**

(22) Filed: **Oct. 19, 2011**

Related U.S. Application Data

(60) Provisional application No. 61/394,640, filed on Oct. 19, 2010, provisional application No. 61/480,154, filed on Apr. 28, 2011.

Publication Classification

(51) **Int. Cl.**

C40B 30/04	(2006.01)
C07K 1/14	(2006.01)
C07K 14/435	(2006.01)
C07K 16/18	(2006.01)
C07K 14/00	(2006.01)

(52) **U.S. Cl.** **506/9**; 530/389.8; 530/391.1; 530/406; 530/395

(57) **ABSTRACT**

Methods for preparing an antibody are provided with the method including incorporating 3-bromo-4-hydroxy-benzoic acid into a protein to form an antigen, immunizing a mammalian host with the antigen, and recovering an antibody having an affinity for the antigen from the host. Antibodies having a binding affinity for a monohalotyrosine are provided as well as composition comprising an antibody bound with monohalotyrosine. Compositions comprising a protein having a 3-bromo-4-hydroxy-benzoic acid moiety are also provided. Methods for evaluating the severity of asthma are provide with the methods including analyzing sputum of a patient using an antibody having a binding affinity for monohalotyrosine, and measuring the amount of antibody bound to protein. Methods for determining eosinophil activity in bodily fluid are also provided with the methods including exposing bodily fluid to an antibody having a binding affinity for monohalotyrosine, and measuring the amount of bound antibody to determine the eosinophil activity.

A. 3-Brominated KLH for immunization

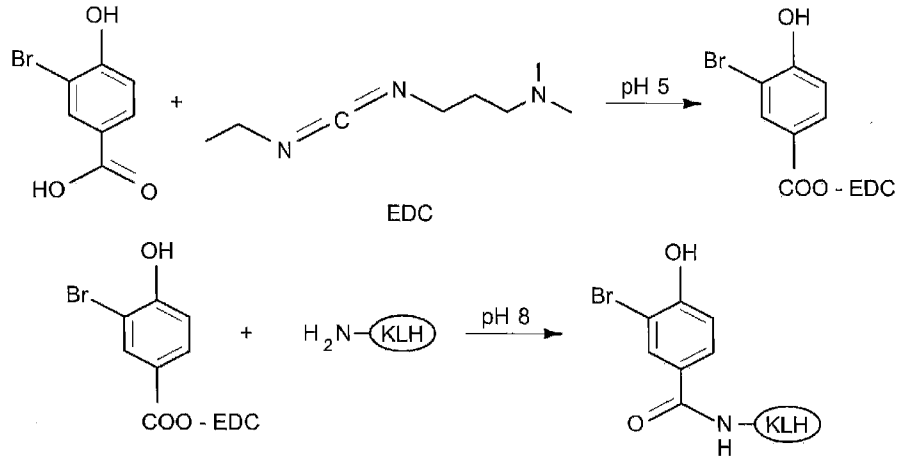

B. NaOBr brominated BSA for screening of antibodies

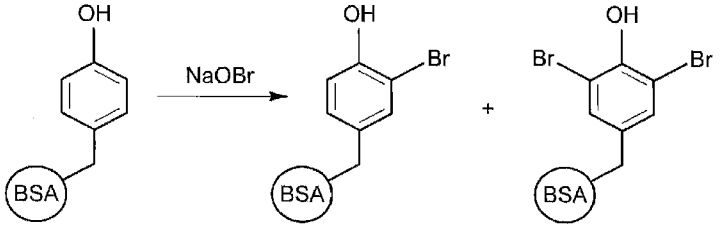

A. 3-Brominated KLH for immunization

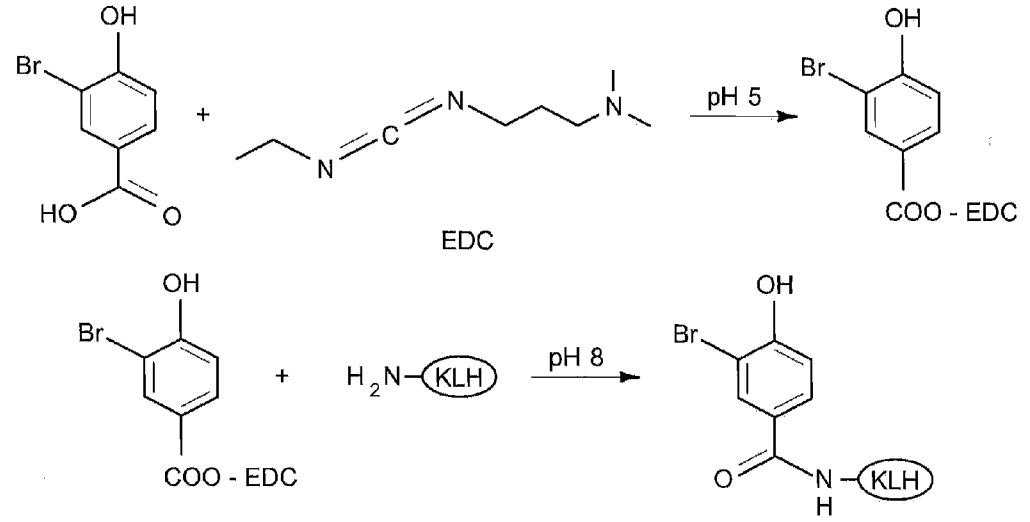

B. NaOBr brominated BSA for screening of antibodies

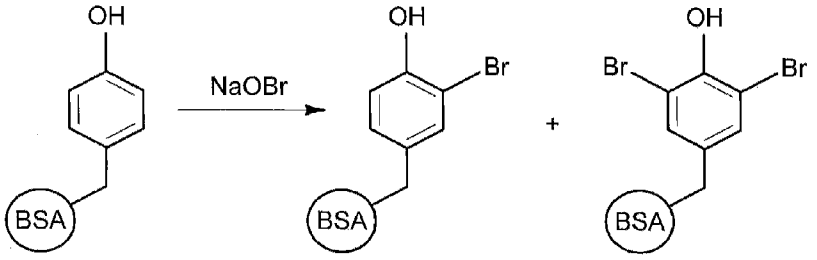

FIG. 1

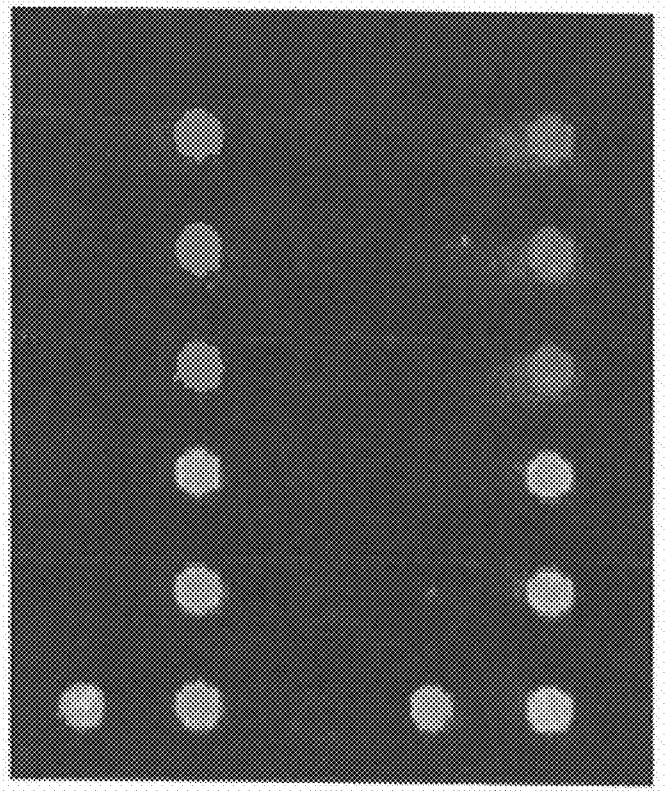

A549	PBS	BSA	BSA	BSA	BSA
BSA-BrO	BSA-BrO	BSA-BrO	BSA-ClO	BSA-ClO	BSA-ClO
BSA-ONOO	BSA-ONOO	BSA-ONOO	BSA-ONOO	BSA-ONOO	BSA-ONOO
A549	PBS	BSA	BSA	BSA	BSA
BSA-BrO	BSA-BrO	BSA-BrO	BSA-ClO	BSA-ClO	BSA-ClO

FIG. 2

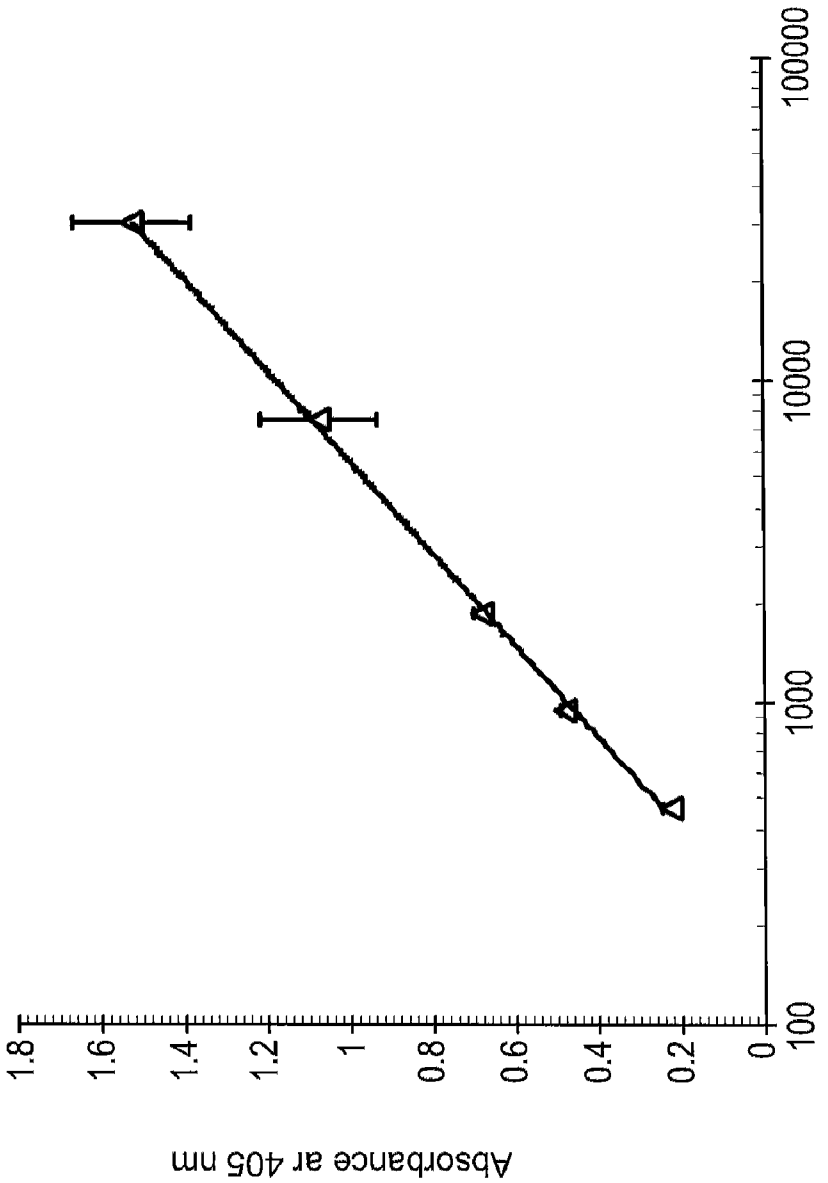
Absorbance ar 405 nm
1.8
1.6
1.4
1.2
1
0.8
0.6
0.4
0.2
0
100
1000
10000
100000
IgM, ng/ml

FIG. 3

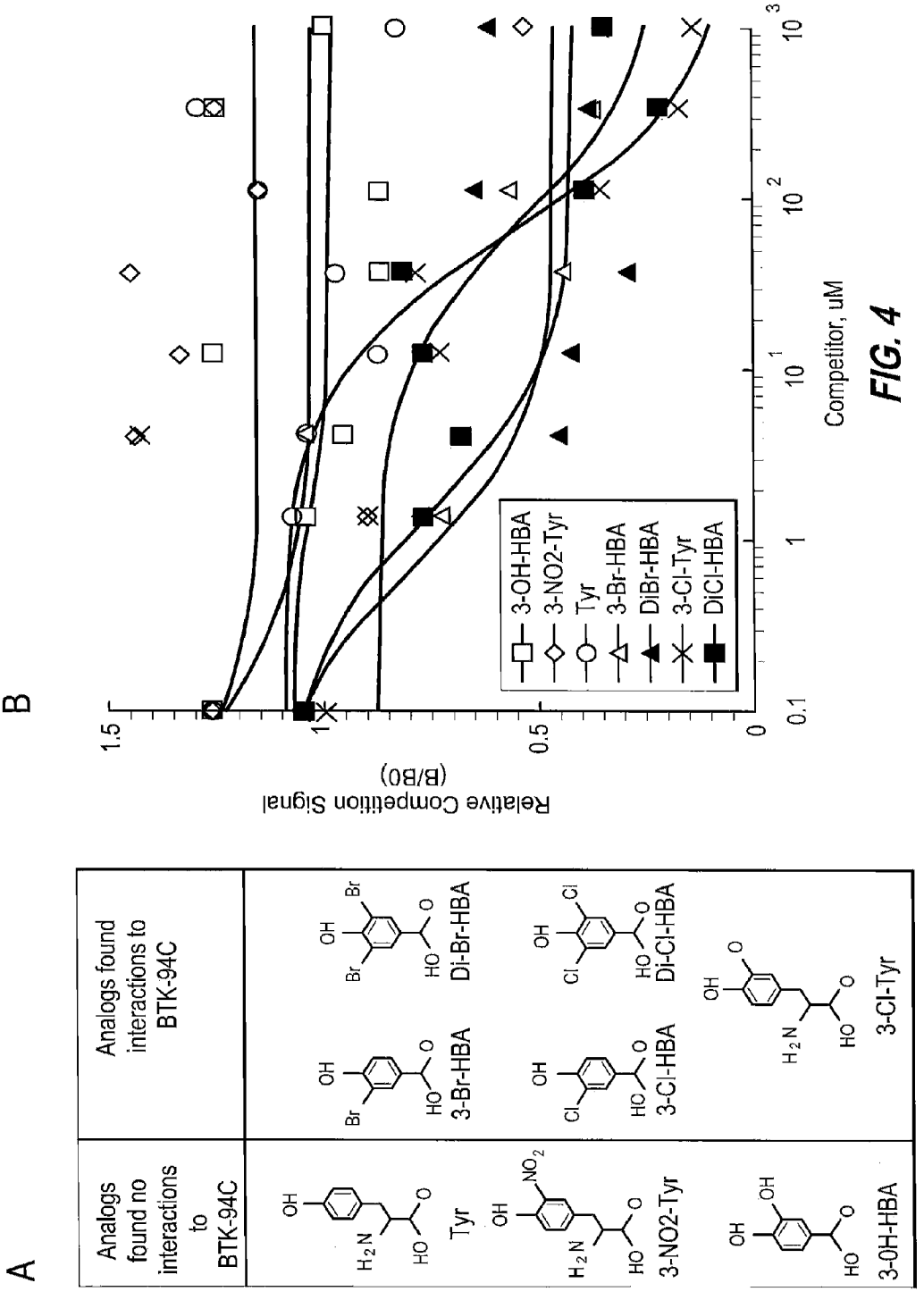
A
Analogs found no interactions to BTK-94C
Tyr
3-NO2-Tyr
3-OH-HBA
Analogs found interactions to BTK-94C
3-Br-HBA
Di-Br-HBA
3-Cl-HBA
Di-Cl-HBA
3-Cl-Tyr
B
Relative Competition Signal (B/B0)
1.5
1
0.5
0
0.1
1
10
10^2
10^3
Competitor, uM
3-OH-HBA
3-NO2-Tyr
Tyr
3-Br-HBA
DiBr-HBA
3-Cl-Tyr
DiCl-HBA

FIG. 4

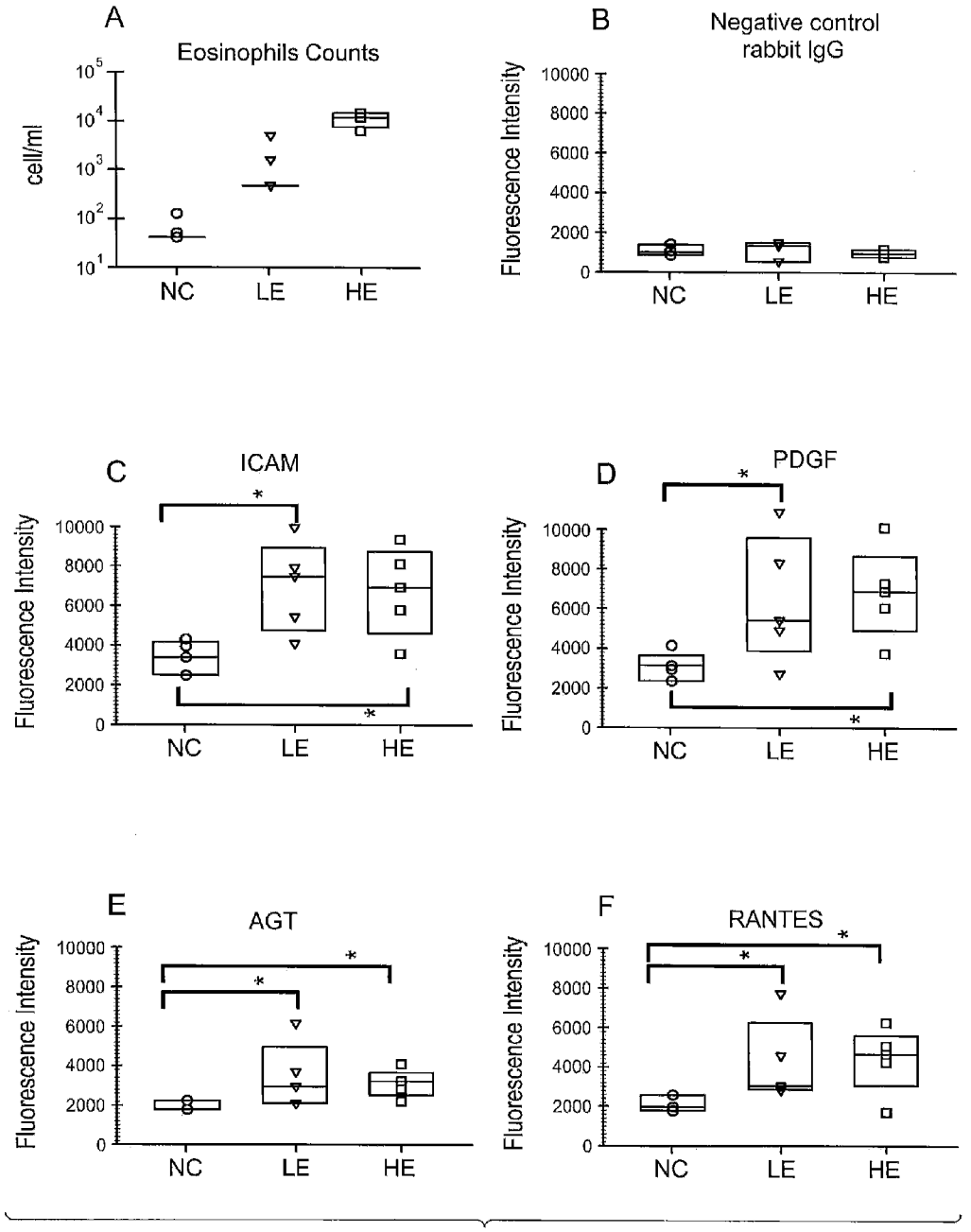
A
Eosinophils Counts
cell/ml
10^5
10^4
10^3
10^2
10^1
NC
LE
HE
B
Negative control
rabbit IgG
Fluorescence Intensity
10000
8000
6000
4000
2000
0
NC
LE
HE
C
ICAM
Fluorescence Intensity
10000
8000
6000
4000
2000
0
*
*
NC
LE
HE
D
PDGF
Fluorescence Intensity
10000
8000
6000
4000
2000
0
*
*
NC
LE
HE
E
AGT
Fluorescence Intensity
10000
8000
6000
4000
2000
0
*
*
NC
LE
HE
F
RANTES
Fluorescence Intensity
10000
8000
6000
4000
2000
0
*
*
NC
LE
HE

FIG. 5

COMPOSITIONS, ANTIBODIES, ASTHMA DIAGNOSIS METHODS, AND METHODS FOR PREPARING ANTIBODIES

CROSS REFERENCE TO RELATED APPLICATIONS

[0001] This application claims priority to U.S. Provisional Application Ser. No. 61/394,640 which was filed on Oct. 19, 2010, and U.S. Provisional Application Ser. No. 61/480,154 which was filed on Apr. 28, 2011, the entirety of each of which are incorporated by reference herein.

GOVERNMENT RIGHTS STATEMENT

[0002] This invention was made with Government support under Contract DE-AC0576RLO1830 awarded by the U.S. Department of Energy. The Government has certain rights in the invention. This research was also supported by the NIEHS Exposure Biology Program (U54/ES016015) and the US Department of Defense breast cancer postdoctoral fellowship W81XWH-10-1-0031.

TECHNICAL FIELD

[0003] The present disclosure relates to the preparation of antibodies and the use thereof. Particular embodiments of the disclosure related to the preparation of antibodies having an affinity for monohalotyrosine and proteins having monohalotyrosine moieties.

BACKGROUND

[0004] Asthma is a common disease that is characterized by an episodic narrowing of the airways. It is a major public health concern that affects about 23 million adults in the United States. Infiltration of activated eosinophils into the bronchioli is believed to be a primary cause of asthma. Eosinophil counts and the presence of secreted eosinophil granular proteins such as Eosinophil Peroxidase (EPO) in sputum and lung biopsy samples are indicators of the severity of asthma. Bromotyrosine protein modifications are increased in asthma patients due to EPO, which catalyzes the formation of hypobromite and the subsequent formation of bromotyrosine. Previous studies that used gas chromatography with mass spectrometric detection found that 3-bromotyrosine and 3,5-dibromotyrosine were significantly elevated in bronchoalveolar lavage fluid and sputum samples from asthmatics, respectively. Studies on the role of brominated proteins in asthma have been limited by the lack of a rapid, simple method to monitor bromotyrosine levels in biofluids.

SUMMARY OF THE DISCLOSURE

[0005] Additional advantages and novel features of the present disclosure will be set forth as follows and will be readily apparent from the descriptions and demonstrations set forth herein. Accordingly, the following descriptions of the present disclosure should be seen as illustrative of the disclosure and not as limiting in any way.

[0006] Bromotyrosine-modified proteins may be useful as stable biomarkers for airway oxidative stress. 3-bromotyrosine is believed to be the predominate bromotyrosine that occurs in vivo; however previous attempts have failed to produce a useful antibody that recognizes 3-bromotyrosine. For example, in 1930, Wormall reported producing rabbit antiserum against 3,5-dibromotyrosine, but failed in his attempt to generate a 3-bromotyrosine antibody. More recently, Kambayashi et al and Kato et al generated polyclonal and monoclonal antibodies against brominated proteins, but their antibodies also only react with 3,5-dibromotyrosine.

[0007] These failures to produce an antibody that recognizes 3-bromotyrosine may arise from the conditions used to produce the antigen. Mass spectrometry and nuclear magnetic resonance analyses indicate that dibromotyrosine modifications are preferentially produced relative to 3-bromotyrosine modifications as a result of in vitro protein bromination. It may be difficult to produce a good antigen for 3-bromotyrosine when using reagents that would be expected to mimic in vivo bromination.

[0008] The present disclosure describes provides antigen compositions that can include a protein having a 3-bromo-4-hydroxy-benzoic acid moiety. The present disclosure also provides methods for producing this antigen.

[0009] From this antigen an antibody having an affinity for halotyrosines can be identified that not only appears to recognize tyrosine residues that are monobrominated, but also binds other halogenated tyrosine residues.

[0010] Methods for producing these antibodies having an affinity for this antigen as well as halotyrosines, including monohalotyrosines, are provided. Antibodies having an affinity for proteins having a halotyrosine moiety are provided as well as compositions that include the antibody bound the halotyrosine.

[0011] Furthermore, the disclosure demonstrates that the disclosed antibody is able to differentiate between levels of halotyrosine in human sputum proteins from healthy controls and asthmatics. Methods for evaluating the severity of asthma are provided as well as methods for determining eosinophil counts.

BRIEF DESCRIPTION OF THE DRAWINGS

[0012] Embodiments of the disclosure are described below with reference to the following accompanying drawings.

[0013] FIG. **1** are synthetic schemes for producing antigens according to an embodiment of the disclosure.

[0014] FIG. **2** is a depiction of an assay according of antibodies produced according to an embodiment of the disclosure.

[0015] FIG. **3** is a depiction of data acquired utilizing antibodies produced according to an embodiment of the disclosure.

[0016] FIG. **4** is a depiction moieties of proteins, and data acquired utilizing antibodies produced according to an embodiment of the disclosure.

[0017] FIG. **5** is a depiction of data acquired utilizing antibodies produced according to an embodiment of the disclosure

DESCRIPTION

[0018] This disclosure is submitted in furtherance of the constitutional purposes of the U.S. Patent Laws "to promote the progress of science and useful arts" (Article 1, Section 8).

[0019] Various advantages and novel features of the present disclosure are described herein and will become further readily apparent to those skilled in this art from the following detailed description. In the preceding and following descriptions, embodiments of the disclosure are provided by way of illustration and description. As will be realized, the disclosure

is capable of modification in various respects without departing from the disclosure. Accordingly, the drawings and description of the embodiments set forth hereafter are to be regarded as illustrative in nature, and not as restrictive.

[0020] The present disclosure provides compositions, antibodies, antigens, methods for producing antigens, methods for producing antibodies, and methods for evaluating asthma, as well as methods of determining eosinophil counts.

[0021] Methods for preparing an antibody are provided. The method can include incorporating a halo tyrosine analog such as 3-bromo-4-hydroxy-benzoic acid into a protein to form an antigen. The method can further include immunizing a mammalian host with the antigen, and recovering an antibody having an affinity for the antigen from the host. In accordance with example implementations the protein can be keyhole limpet hemocyanin (KLH). In accordance with this method a composition includes an antigen provided by modifying KLH with a compound that mimics 3-bromotyrosine. Accordingly a composition is provided that can include a protein having a 3-bromo-4-hydroxy-benzoic acid moiety, with the protein being KLH, for example.

[0022] In accordance with aspects of the disclosure, this can avoid the problem associated with in vitro protein bromination and the production primarily of dibromotyrosine. Bovine Serum Albumin (BSA) can then be brominated under conditions to optimize monobromination, and then used to screen hybridoma cell lines and to identify a clone that can have an affinity for physiologically relevant tyrosine modifications. This resulting BTK-94C antibody has an affinity for 3-bromotyrosine and 3,5-dibromotyrosine, also has an affinity for 3-chlorotyrosine and 3,5-dichlorotyrosine, but has no affinity for unmodified tyrosine, 3-nitrotyrosine or 3-hydroxytyrosine (see, e.g., FIGS. **2** and **4**).

[0023] Chlorotyrosine modifications of proteins are also provided using hypochlorite, a product of myeloperoxidase, which is an enzyme found in neutrophil and macrophages. Because this antibody appears to bind all four physiologically relevant halogenated protein tyrosine residues, BTK-94C may be considered a general halotyrosine antibody.

[0024] Accordingly, methods of the disclosure provide an antibody having a binding affinity for protein halotyrosines and in particular embodiments, monohalotyrosine. The halotyrosine can be one or both of a monohalotyrosine and/or a dihalotyrosine. The monohalotyrosine can one or both of bromotyrosine and/or chlorotyrosine. The monohalotyrosine can also be one or both of 3-bromotyrosine and/or 3-chlorotyrosine. The dihalotyrosine can be one or both of 3,5-dibromotyrosine and/or 3,5-dichlorotyrosine. Compositions are also provided that include the antibody of the present disclosure bound to the antigen, with the antigen being the halotyrosine and/or halotyrosine protein.

[0025] Example implementations using antibodies of the present disclosure can overcome various problems associated with the previously used methods. Although there have been several polyclonal and monoclonal antibodies reported to react with brominated proteins, those antibodies appear to only react with dibromotyrosine, and not with 3-bromotyrosine. As 3-bromotyrosine is the predominate modification observed in vivo, this is an important limitation.

[0026] The present disclosure further provides methods that can include exposing the antibody to bodily fluid to determine one or more of eosinophil activity, inflammation, and/or an amount of protein having a monohalotyrosine and/or a dihalotyrosine moiety, for example.

[0027] Methods are also provided for evaluating the severity of asthma. The methods can include comprising analyzing sputum of a patient using an antibody having a binding affinity for monohalotyrosine, and measuring the amount of antibody bound to protein. The method can be one or both of qualitative and/or quantitative. The method can include correlating the amount of bound antibody to determine the amount of inflammation. The method may separately or together, include using the amount of bound antibody to monitor drug responses to asthma attacks.

[0028] Methods are also provided for determining eosinophil activity in bodily fluid. The methods can include exposing bodily fluid to an antibody having a binding affinity for monohalotyrosine, and measuring the amount of bound antibody to determine the eosinophil activity. The bodily fluid can be sputum or lavage fluid, for example. The method can also include correlating the amount of bound antibody to determine inflammation and/or drug responses, for example.

[0029] Accordingly, BTK-94C was tested with human sputum samples collected from asthmatics and healthy controls. An ELISA microarray analysis demonstrated that 4 proteins in human sputum samples are halogenated at increased levels in asthmatics. These data indicate that bromination is a specific indicator of eosinophil activity and that 4 specific proteins are modified in response to asthma-related eosinophil activity. Further, halogenation levels of these proteins may be useful in monitoring asthma.

[0030] Below is described a novel monoclonal antibody (BTK-94C) that recognizes brominated and chlorinated proteins. These halotyrosine protein modifications are indicative of inflammatory cell activity. This antibody was used as a detection reagent in sandwich ELISAs to demonstrate that halotyrosine levels of four sputum proteins are increased in asthmatics. Thus, the BTK-94C antibody can provide an indication of inflammation in asthmatics, and these ELISAs can prove useful for predicting or monitoring drug responses in asthma or in other diseases with a strong inflammatory component.

Example Materials and Methods

[0031] Bovine serum albumin (BSA) was purchased from Jackson ImmunoResearch Laboratory. 3-bromo-4-hydroxybenzoic acid was purchased from Indofine Chemical Company Inc. 3,5-dibromo-4-hydroxybenzalehyde, 3,5-dichloro-4-hydroxybenoic acid, 3,4-dihydroxybenic acid, 3-nitrotyrosine and L-tyrosine were purchased from Sigma-Aldrich. Keyhole limpet hemocyanin (KLH), 1-ethyl-3-(3-dimethylaminopropyl) carbodiimide (EDC), ascites conditioning reagent, Melon monoclonal antibody purification kit, and biotinylation kit EZ-link sulfo-NHS-biotin were purchased from Pierce-Thermo Scientific (Rockford, Ill.). Sodium hypobromite solution was purchased from Fisher-Thermo Scientific. Capture antibodies for 23 ELISA were purchased as stated in the supplementary data.

Example Preparation of the Brominated Antigen and Related Modified Proteins

[0032] For the preparation of the antigen, a modified protocol of the carbodiimide method as described in "*A Simple Modified Carbodiimide Method for Conjugation of Small-Molecular-Weight Compounds to Immunoglobulin G with Minimal Protein Crosslinking*", Minh-Tam B. Davis and James F. Preston, *Analytical Biochemistry* 116, 402-407

(1981), which is incorporated by reference herein, was used. Briefly, 0.12 mM 3-Br-HBA was dissolved in 2.5 ml methanol and combined with 0.75 mM EDC in 2.5 ml of 20 mM potassium phosphate buffer (pH 5.0) at room temperature for 2 min. This 5 ml solution was then mixed with 8 ml of 2.5 mg/ml KLH in 200 mM potassium phosphate buffer (pH 8.0) and allowed to incubate overnight at room temperature. Any remaining EDC and 3-Br-HBA were removed by dialysis against 120 mM PBS at 4° C. After dialysis, a precipitate was removed by centrifuge at 50,000 g for 2 h at 4° C. The modified antigen, in pH 8.0, 200 mM potassium phosphate buffer, was quantified by measuring the absorbance at 280 nm for protein concentration and 310 nm for bromination. The modified KLH was aliquotted and stored at −80° C. Mice were immunized, serum collected, and hybridoma cell lines and their supernatants, ascites production, and antibody isotyping was undertaken at the Washington State University Monoclonal Antibody Center (Pullman). The BTK-94C antibody was biotinylated using the EZ-Link Sulfo-NHS-LC-Biotinylation Kit (Pierce, Rockford, Ill.), according to the manufacturer's protocol.

[0033] Brominated BSA was prepared using sodium hypobromite (Fisher Scientific, Pittsburgh, Pa.), as previously reported. To maximize the amount of 3-bromotyrosine relative to 3,5-dibromotyrosine, we used optimized conditions, as previously reported. That is, 1 ml of 10 mg BSA/ml was reacted with 200 μl of freshly prepared 20 mM sodium hypobromite (in pH 7.2 PBS) at 25° C. for 15 h. The solution was then dialyzed against PBS at 4° C. to remove unreacted reagents. To generate chlorinated BSA and nitrated BSA, 6% sodium hypochlorite (The Clorox Company) and peroxynitrite (Millipore Corporation, Boston, Mass.) were used, respectively, as previously reported.

Example, ELISA Microarray Assay and Inhibition Studies with Modified Tyrosine Analogs.

[0034] Sandwich ELISA microarray was performed as previously described except that the initial biotin signal was generated by goat-anti-mouse-IgM conjugated to horseradish peroxidase (Jackson ImmunoResearch Laboratories) in combination with biotinyltyramide. In brief, after centrifugation to remove any particulates, sputum samples were diluted 5-fold in 0.1% BSA in PBS. 25 μl of each diluted sample/chip was analyzed on three chips. Each chip contained 4 replicate spots for each capture antibody, such that there are a total of 12 replicates/sample for each of the 23 ELISAs. (See, e.g, Table 1 Below)

TABLE S1

Selected plasma biomarkers and references that relate these proteins to asthma.

Capture antibodies	Abbreviation	Catalog # and Source
alpha-lactalbumin	a-LB	Sc-58672 [2]
amphiregulin	AmR	MAB262 [1]
ceruloplasmin	CP	sc-69767 [2]
C-reactive protein	CRP	MAB17071 [1]
epidermal growth factor (EGF)	EGF	DY236 kit [1]
EGF receptor	EGFR	AF-231 [1]
E-selectin	Esel	AF-724 [1]
basic fibroblast growth factor	FGFb	MAB233 [1]
fibrinogen	Fibr	ID6-250310 [3]
heparin-binding epidermal growth factor	HBEGF	AF-292 [1]

TABLE S1-continued

Selected plasma biomarkers and references that relate these proteins to asthma.

Capture antibodies	Abbreviation	Catalog # and Source
hepatocyte growth factor	HGF	MAB694 [1]
intracellular adhesion molecular 1	ICAM	MAB720 [1]
insulin-like growth factor 1	IGF-1	MAB291 [1]
leptin	Leptin	MAB398 [1]
matrix metalloprotease 1	MMP1	AF901 [1]
matrix metalloprotease 2	MMP2	AF902 [1]
matrix metalloprotease 9	MMP9	AF911 [1]
platelet-derived growth factor A	PDGF	MAB221 [1]
RANTES	RANTES	MAB678 [1]
surfactant protein A	SP-A	LS-C17957 [4]
transforming growth factor alpha	TGFa	AF-239 [1]
tumor necrosis factor alpha	TNFa	MAB610 [1]
vascular endothelial growth factor	VEGF	AF-293 [1]

[1] R&D Systems; Minneapolis, MN, USA.
[2] Santa Cruz Biotechnology, Inc, Santa Cruz, CA USA.
[3] ABBiotek, San Diego CA , USA
[4] Lifespan Biosciences, Seattle WA, USA.

[0035] For the microarray assays to define antibody binding characteristics, modified and unmodified proteins were individually printed on aminopropylsilane-coated slides. The slides were then blocked with 2% BSA in PBS. 50 μL of the hybridoma supernatant was preincubated with 50 μL of a specific concentration of a chemical competitor (in 0.1% BSA/PBS) at room temperature for 12 h. Individual chemical competitors were serially diluted prior to mixing with the hybridoma supernatant. 25 μL of the mixture were loaded onto each microarray chip prior to incubation at room temperature for 16 h. The plate was washed three times with 0.05% Tween-20 in PBS, as previously described. The biotin signal was detected with streptavidin conjugated to Cy3, and then imaged using a ScanArray Express HT laser scanner (Perkin-Elmer, Downer Grove, Ill.). ScanArray Express software was used to analyze the images and determine the spot fluorescent signal.

Example ELISA Microarray

[0036] The printing and processing of the ELISA microarray chips has been previously described in detail in "*An Internal Calibration Method for Protein-Array Studies*", Don Simone Daly, et al, *Statistical Applications in Genetics and Molecular Biology,* Volume 9, Issue 1, 2010, Article 14, which is incorporated by reference herein. Green fluorescent protein (100 pg/mL) was spiked into each sputum sample and analyzed on the chip using a sandwich ELISA with separate capture and detection antibodies. Data from this analysis were used to normalize the data from the other ELISAs using ProMAT Calibrator, a custom bioinformatics program that we developed specifically for this purpose as described in "*An Internal Calibration Method for Protein-Array Studies*", Don Simone Daly, et al, *Statistical Applications in Genetics and Molecular Biology,* Volume 9, Issue 1, 2010, Article 14, and "*Preparation and Characterization of a Polyclonal Antibody Against Brominated Protein*", Yasuhiro Kambayashi, et al., *J. Clin. Biochem. Nutr.* 44, 95-103, January 2009, the entirety of each of which are incorporated by reference herein. ProMAT Calibrator is freely available at www.pnl.gov/statistics/Pro-

MAT/. The procedures used for processing the microarray chips were essentially identical to those previously reported in "*An Internal Calibration Method for Protein-Array Studies*", Don Simone Daly, et al, *Statistical Applications in Genetics and Molecular Biology,* Volume 9, Issue 1, 2010, Article 14, except that only a single detection antibody was used.

[0037] In brief, each capture antibody was printed onto each chip in quadruplicate spots, once in each quadrant of the chip. In addition, antibodies for the GFP and orientation spots were printed in quadruplicate on each chip. Individual chips were incubated with one diluted sputum sample, and each sample was analyzed on three chips. The biotinylated halotyrosine monoclonal antibody that is described above (BTK-94C) was used to detect 3-bromotyrosine in the captured antigens. The processed slides were imaged with a ScanArray Express HT laser scanner (Perkin-Elmer, Downer Grove, Ill., USA) and ScanArray Express software was used to analyze the images and determine spot fluorescent intensity.

Example Statistics

[0038] Statistical comparisons were made using one-way analysis of variance {Chambers, 1992), when statistically significant, Tukey's Honest Significant Difference method was used to define which asthma groups had elevated levels of bromotyrosine. A probability value of $p<0.05$ was used to delineate statistical significance for all analyses.

Example Results

Evaluation of a Monoclonal Antibody for Halotyrosine.

[0039] Hypobromite reacts with protein tyrosines to produce both 3-bromotyrosine and 3,5-dibromotyrosine modifications (FIG. **1**B). Procedures used for developing antigens containing either 3-brominated tyrosine or a related protein modification. A. Conjugation of 3-bromobenzoic acid to protein, as was used for generating the KLH antigen that was used for immunizing mice; B. Diagram of how sodium hypobromite is believed to modify tyrosine residues in vivo. This same chemistry was used to generate a modified BSA antigen that was used for screening hybridoma cell lines. Although the 3,5-dibromotyrosine modification predominates for the in vitro reaction, 3-bromotyrosine predominates in vivo. Thus, the fact that previous antibodies generated against in vitro brominated antigens only recognize the dibrominated tyrosine modifications suggests that this failure may reflect the antigen. For an antigen, a protein modification mimicing 3-bromotyrosine, namely a 3-bromo-4-hydroxy-benzonic-acid adducted to KLH was used. As such, it was confirmed that this artificial antigen produced antibodies that recognize a physiologically relevant brominated protein modification. Antibodies recovered from the serum from the mice immunized with the modified KLH antigen were found that did bind with brominated BSA, but not unmodified BSA (data not shown), indicating that the bromotyrosine mimic did result in antibodies that reacted with biologically relevant protein modifications.

[0040] The immunized mice were then used to generate 225 monoclonal hybridoma cell lines. Supernatants from these cultured cell lines were tested for reactivity and specificity using a custom protein microarray chip that contained individual spots of brominated BSA, chlorinated BSA, nitrated BSA, and unmodified BSA. These tests demonstrated that the BTK-94 antibody strongly reacted with brominated BSA, weakly reacted with chlorinated BSA, but did not react with unmodified BSA or nitrated BSA (FIG. **2**).

[0041] FIG. **2** demonstrates the evaluation of recognition pattern of BTK-94C with different in vitro modified BSA. Left: pattern of antigens printed on the slide. Spot diameters are approximately 200 microns. Right: Cy3-scanned fluorescence image showing binding pattern of BTK-94C. A543, antibody modified with Alexa 543, which is used as an orientation spot; BSA-BrO, hypobromite-treated BSA; BSA-ClO hypochlorite-treated BSA; BSA-ONOO: peroxynitrite treated BSA.

[0042] This hybridoma cell line was further cultured to ensure that it was truly monoclonal. The BTK-94C antibody that is used in all subsequent tests was derived from these monoclonal cell lines. Tests indicated that this antibody had the same binding characteristics as shown for BTK-94 (FIG. **2**).

Example Preparation and Characterization of Monoclonal Antibodies to Brominated Proteins.

[0043] Isotyping of the BTK-94C indicated that this is an IgM antibody and reacted with brominated BSA in a concentration-dependent manner (FIG. **3**). In FIG. **3**, the signal produced with brominated BSA correlates with the concentration of the BTK-94C antibody. The ascites fluid from this cell line was also analyzed for specificity and cross-reactivity using protein microarray analysis. Consistent with results from hybridoma supernatants (see above), the BTK-94C antibody produced in the ascites bound brominated and chlorinated BSA, but no reactivity with unmodified or peroxynitrite-treated BSA was observed (data not shown), further confirming that this antibody preferentially reacts with halogenated proteins.

[0044] To further characterize the specificity of this antibody, the ability of reagents that mimic tyrosine modifications to inhibit the BTK-94C antibody binding to brominated BSA was evaluated. The binding of BTK-94C to brominated BSA was strongly inhibited by 3-bromo-4-hydroxybenzoic acid and 3,5-dibromo,4-hydroxybenzoic acid, but less potently inhibited by 3-chlorotyrosine and 3,5-dichloro,4-hydroxybenzoic acid (FIG. **4**B). Binding to brominated BSA was not inhibited by intact tyrosine, 3-nitrotyrosine or 3,4-dihydroxybenzoic acid (FIG. **4**).

[0045] Referring to FIG. **4**, binding properties of BTK-94C to brominated albumin based on inhibition by modified tyrosine analogs is shown. The individual chemicals and BTK-94C were incubated overnight and then added to protein microarray chips printed with brominated BSA. Abbreviations and related chemical names and structures are shown in panel A: 3-Br-HBA, 3-bromo-4-hydroxybenzoic acid; DiBr-HBA, 3,5-dibromo-4-hydroxybenzalehyde, DiCl-HBA, 3,5-dichloro-4-hydroxybenoic acid, 3-OH-HBA3,4-dihydroxybenic acid, 3-NO2-Tyr, 3-nitrotyrosine and Tyr, L-tyrosine. Panel B: The results were expressed as relative competition as B/B0, where B is the amount of antibody bound in the presence of competitor and B0 is the amount in the absence of the competitor. Each point represents the median of triplicate analyses. These results further suggest that BTK-94C recognizes 3-bromotyrosine as well as chlorotyrosine protein modifications.

Example BTK-94C Analysis of Halogenated Tyrosine Modifications in Human Sputum Proteins.

[0046] To determine if this antibody has potential for evaluating eosinophil activity in asthmatics, an ELISA microarray

platform was utilized that employed BTK-94C as the sole detection antibody. On this ELISA chip, were printed 23 capture antibodies for antigens that are potentially related to asthma (see supplementary data). Of these captured antigens, a statistically significant increase in the bromination levels of AGT, ICAM, PDGF and RANTES in asthmatics with either high eosinophil or low eosinophils counts in the sputum samples when compared to the healthy controls was observed. (FIG. **5**).

[0047] Referring to FIG. **5**, halogenated proteins are elevated in protein present in sputum from asthmatics. (A). Eosinophils counts from sputum samples tested in this study. (B) Nonimmune rabbit IgG was printed onto the ELISA microarray as a negative control spot showed completely flat signal through all tested sputum samples. Halotyrosine levels for intracellular adhesion molecular 1 (ICAM) (C), platelet-derived growth factor AA (PDGF) (D), AGT (E), and RANTES (F). The lateral line represents the median values, and boxes are the 25^{th} and 75 quantile's.

[0048] Data from ELISA microarray analysis indicates significantly different ($p<0.05$) based on ANOVA and Turkey's test. In contrast, the other 19 assays that were performed with this chip did not show any significant differences. For the ELISA microarray analysis, nonimmune rabbit IgG was printed as a negative control. The signal from this spot was low in comparison to others, and there were no treatment-related changes in this signal (FIG. **5**B), suggesting that the differential signal associated with asthma that was observed in the spots containing capture antibodies was due to differential halogenation of the captured antigens.

[0049] In compliance with the statute, embodiments of the disclosure have been described in language more or less specific as to structural and methodical features. It is to be understood, however, that the entire disclosure is not limited to the specific features and/or embodiments shown and/or described, since the disclosed embodiments comprise forms of putting the disclosure into effect. The disclosure is, therefore, claimed in any of its forms or modifications within the proper scope of the appended claims appropriately interpreted in accordance with the doctrine of equivalents.

1. An antibody having a binding affinity for a monohalotyrosine.

2. The antibody of claim **1** wherein the monohalotyrosine is bromotyrosine.

3. The antibody of claim **1** wherein the monohalotyrosine is chlorotyrosine

4. The antibody of claim **1** wherein the monohalotyrosine is a moiety of a protein.

5. The antibody of claim **1** wherein the antibody also has a binding affinity for dihalotyrosine.

6. A composition comprising an antibody bound with monohalotyrosine.

7. The composition of claim **6** wherein the monohalotyrosine is a moiety of a protein.

8. The composition of claim **6** wherein the monohalotyrosine is one or both of bromotyrosine and/or chlorotyrosine.

9. A composition comprising a protein having a 3-bromo-4-hydroxy-benzoic acid moiety.

10. The composition of claim **9** wherein the protein is keyhole limpet hemocyanin (KLH).

11. A method for evaluating the severity of asthma comprising:

analyzing sputum of a patient using an antibody having a binding affinity for monohalotyrosine; and

measuring the amount of antibody bound to protein.

12. The method of claim **11** wherein the measuring is one or both of qualitative and/or quantitative.

13. The method of claim **11** wherein the monohalotyrosine is a moiety of a protein.

14. The method of claim **11** wherein the monohalotyrosine is one or both of bromotyrosine and/or chlorotyrosine.

15. The method of claim **11** further comprising correlating the amount of bound antibody to determine the amount of inflammation.

16. The method of claim **11** further comprising using the amount of bound antibody to monitor drug responses to asthma attacks.

17. A method for determining eosinophil activity in bodily fluid, the method comprising:

exposing bodily fluid to an antibody having a binding affinity for monohalotyrosine; and

measuring the amount of bound antibody to determine the eosinophil activity.

18. The method of claim **17** wherein the bodily fluid is sputum.

19. The method of claim **17** wherein the monohalotyrosine is a moiety of a protein.

20. The method of claim **17** wherein the monohalotyrosine is one or both of bromotyrosine and/or chlorotyrosine.

21. The method of claim **17** further comprising correlating the amount of bound antibody to determine inflammation and/or drug responses.

22. A method for preparing an antibody, the method comprising:

incorporating 3-bromo-4-hydroxy-benzoic acid into a protein to form an antigen;

immunizing a mammalian host with the antigen; and

recovering an antibody having an affinity for the antigen from the host.

23. The method of claim **22** wherein the protein is keyhole limpet hemocyanin (KLH).

24. The method of claim **22** wherein the antibody has a binding affinity for monohalotyrosine.

25. The method of claim **24** wherein the monohalotyrosine is one or both of bromotyrosine and/or chlorotyrosine.

26. The method of claim **22** wherein the antibody has a binding affinity for protein halotyrosines.

27. The method of claim **26** wherein the halotyrosine is one or both of a monohalotyrosine and/or a dihalotyrosine.

28. The method of claim **27** wherein the monohalotyrosine is one or both of 3-bromotyrosine and/or 3-chlorotyrosine.

29. The method of claim **27** wherein the dihalotyrosine is one or both of 3,5-dibromotyrosine and/or 3,5-dichlorotyrosine.

30. The method of claim **22** further comprising exposing the antibody to bodily fluid to determine eosinophil activity.

31. The method of claim **22** further comprising exposing the antibody to bodily fluid to determine inflammation.

32. The method of claim **22** further comprising exposing the antibody to bodily fluid to determine an amount of protein having a monohalotyrosine and/or a dihalotyrosine moiety.

* * * * *